Antenna Designs for CubeSats: A Review

SUHILA ABULGASEM[1], (Student Member, IEEE),
FAISEL TUBBAL[1,2], (Senior Member, IEEE),
RAAD RAAD[1], (Member, IEEE),
PANAGIOTIS IOANNIS THEOHARIS[1], (Student Member, IEEE),
SINING LU[1], (Student Member, IEEE), AND SAEID IRANMANESH[1]

[1]School of Electrical, Computer and Telecommunication Engineering, University of Wollongong, Wollongong, NSW 2522, Australia
[2]Technological Projects Department, Libyan Center for Remote Sensing and Space, Tripoli 21218, Libya

Corresponding author: Faisel Tubbal (faisel@uow.edu.au)

ABSTRACT Cube Satellites, aka CubeSats, are a class of nano satellites that have gained popularity recently, especially for those that consider CubeSats as an emerging alternative to conventional satellites for space programs. This is because they are cost-effective, and they can be built using commercial off-the-shelf components. Moreover, CubeSats can communicate with each other in space and ground stations to carry out many functions such as remote sensing (e.g., land imaging, education), space research, wide area measurements and deep space communications. Consequently, communications between CubeSats and ground stations is critical. Any antenna design for a CubeSat needs to meet size and weight restrictions while yielding good antenna radiation performance. To date, a limited number of works have surveyed, compared and categorised the proposed antenna designs for CubeSats based on their operating frequency bands. To this end, this paper contributes to the literature by focusing on different antenna types with different operating frequency bands that are proposed for CubeSat applications. This paper reviews 48 antenna designs, which include 18 patch antennas, 5 slot antennas, 4 dipole and monopole antennas, 3 reflector antennas, 3 reflectarray antennas, 5 helical antennas, 2 metasurface antennas and 3 millimeter and sub-millimeter wave antennas. The current CubeSat antenna design challenges and design techniques to address these challenges are discussed. In addition, we classify these antennas according to their operating frequency bands, e.g., VHF, UHF, L, S, C, X, Ku, K/Ka, W and mm/sub-mm wave bands and provide an extensive qualitative comparison in terms of their size, −10 dB bandwidths, gains, reflection coefficients, and deployability. The suitability of different antenna types for different applications as well as the future trends for CubeSat antennas are also presented.

INDEX TERMS CubeSats, planar antennas, helical antennas, radiation patterns, gain, dipole antennas, reflect array antennas, reflection coefficient.

I. INTRODUCTION

For many years, Medium Earth Orbit (MEO) satellites were the only option for satellite industry and space organizations. As set out in Table 1, MEO satellites have a mass ranging from 500 to 1000 kg, operate at altitude of 900 km, are sun synchronous and consume high power, i.e., 8kW. Their typical timeframe is about four years and their cost ranges between 50 to 100 million US dollars [1]. Therefore, they have always been constructed by large companies and government organizations who can afford the cost of building and operation of such large satellites. Moreover, they are used for

different applications including remote sensing (e.g., weather forecasting) and communications (e.g., mobile telephony and scientific observation). An example of MEO conventional satellite is Formosat-2, which is the first sun-synchronous remote sensing satellite and scientific observation program that was built and used by National Space Program Office (NSPO) in Taiwan [2]. It was launched in 2004 to operate at an altitude of 891 km and used for disaster preparedness, rescue, and environment monitoring. These types of conventional satellites use heavy medium-gain antennas such as horn antennas with a precise pointing mechanism to communicate with the ground station.

In contrast, Cube Satellites (CubeSats) are a cost-effective option for the satellite industry, which have become

accessible to the public. CubeSats operate at Low Earth Orbit (LEO), are small, are lightweight and can be built using Commercial Off-The-Shelf (COTS) components [3], [4]. Fig. 1 (a), (b) and (c) shows three common types of CubeSats with different sizes: (10cm × 10cm × 10cm), (10cm × 10cm × 20cm) and (10cm × 10cm × 30cm) for 1U, 2U and 3U CubeSats, respectively. Their mass ranges from 1 to 6 kg and are low power, e.g., 2 W. As set out in Table 1, compared to medium satellites, CubeSats are cheaper, have smaller size, consume less power and take less time to build and correspondingly have much more limited functionality. One example of a CubeSat is the Tokyo Tech 1U CubeSat called CUTE-I which was designed by Tokyo institute of technology in 2003 [5]. CUTE-I had a mass of 1kg, operated at LEO of 820 km and was developed for communication and attitude sensing missions.
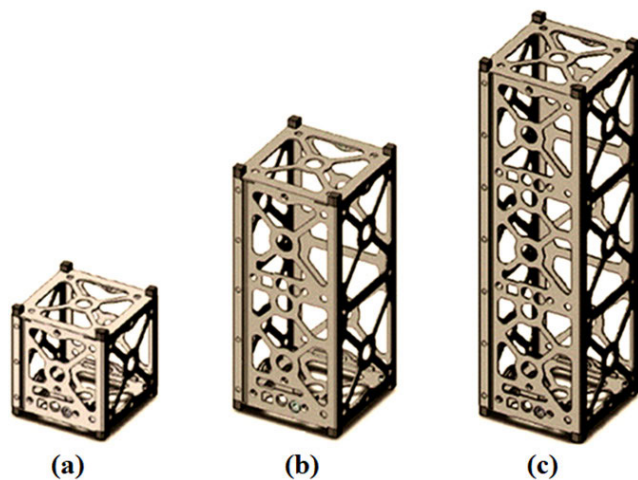

FIGURE 1. Cube satellite models, (a) 1U, (b) 2U and (c) 3U.

TABLE 1. Comparison between MEO conventional satellites and LEO cube satellites.

Type	Mass (kg)	Cost (US $)	Time to Build	Power Consumption
Conventional	500-1000	50-100 M	4 years	~ 800 W
CubeSat	1-6	20-200 K	<1 year	~2 W

One of the main subsystems of CubeSat is the Telemetry, Tracking and Communications (TTC) subsystem. The main function of TTC subsystem is to provide reliable communication links between CubeSats and ground station. This is important as it ensures continuous communication between the ground station and the CubeSat. A key component of the communication subsystem is the antenna. Antennas on Cube-Sat are used to send telemetry and science data (i.e. images) from CubeSat to ground station and to receive commands from ground station to CubeSat. However, designing such

antennas is a challenge as the antenna needs to meet several restrictions related to the CubeSat's size, i.e., ≤10 × 10 × 10 cm^3, weight, i.e., ≤1.3 kg, and power, i.e., ≤2 W while yielding high gain and wide bandwidth [6]. Fig. 7 shows some examples of different antenna types that were designed and proposed for CubeSat applications. These antenna designs include patch, slot, helical, monopole, reflectarrays, mesh reflectors and metasurface antennas.

A. RELATED REVIEW ARTICLES ON CUBESAT ANTENNAS

The first study/review on CubeSat antennas were published by the authors of this paper in 2015 and can be found in [4]. The authors investigated the suitability of planar antenna designs for CubeSat missions due to their low profile, small size, and gain performance. The authors also provide a qualitative evaluation of suitable planar antenna designs and a quantitative comparison of the four most suitable planar antenna designs for CubeSat at the time. Following that, in 2017, the authors in [7] and [8] grouped the most popular CubeSat antenna designs and categorized them according to their types. The most popular antenna types for CubeSat applications were found to be planar (patch), monopole/dipoles, reflectors, reflectarrays, helical and horn antennas. As CubeSats were gaining popularity among the space enthusiasts, in 2018, different CubeSat antennas were studied based on the mission suitability and their subsystem usage [9]. More specifically, different antenna types were identified for high data rate downlink, Synthetic Aperture Radar (SAR), inter-satellite links (ISL), navigation and remote sensing applications. Moreover, CubeSats have also been considered for deep space missions. In 2019, a summary of CubeSat antennas that are suitable for deep space missions with a focus on their gains and operating frequencies are presented in [10]. The advantages and disadvantages of different antenna types, e.g., reflectarrays, metasurfaces, inflatable, membrane, mesh reflectors and slot/patch arrays that are suitable for deep space communications in terms of their stowage volume, efficiency, and Technology Readiness Level (TRL) were highlighted. A summary of the review articles associated with CubeSat antennas can be found in Table 2.

B. CONTRIBUTION OF THIS PAPER

This paper presents an extensive and comprehensive literature survey of antenna designs that are *only designed and proposed for CubeSats* with design techniques and approaches to achieve high gain, wide bandwidth, circular polarization and small size. Other studies have covered some standard antenna designs that have been adapted for CubeSats. It has been noted that different types of antennas that are designed, proposed and used for CubeSats' communications have not yet been compared and evaluated in terms of their performance. Hence, we first present and classify antenna designs with different operating frequencies based on their type. The CubeSat application of each antenna design as well as an evaluation in terms of its gain, bandwidth, size and polarization is provided. Then, the current challenges of CubeSat antennas

TABLE 2. Existing review articles on CubeSat antennas.

Reference	Year	Antennas categorized or studied based on
Tubbal *et al.* [4]	2015	*Planar antenna design techniques, approaches, and their suitability for CubeSat missions*
Rahmat-Samii *et al.* [7]	2017	*Antenna types*
Lokman *et al.[8]*	2017	*Antenna types, materials used and deployment mechanisms*
Gao *et al.* [9]	2018	*Missions and CubeSat subsystem compatibility*
Chahat *et al.* [10]	2019	*Gain and frequency and suitability for CubeSat Deep Space missions*
This paper	2020	*Antenna type/operating frequency/approach and qualitative performance comparison in terms of gain, bandwidth, size and deployability.*

namely, high gain, wide bandwidth, multi-band, small size, low mass, and circular polarization are identified. Additionally, to address those challenges, different approaches used in the literature are investigated. Each approach is categorized based on its suitability for different antenna types. We have also classified the antennas according to their operating frequency bands and compare their performance. Finally, we provide the future trends on antenna designs for emerging CubeSat applications.

The remainder of this paper has the following structure. Sections II, III, IV, V and VI present a comprehensive taxonomy of the main challenges and solutions in designing different antenna types at different operating frequencies for different CubeSat applications. We classify them according to their types. In Section VII, the current CubeSat challenges are identified, and different approaches are analyzed based on the challenge they address and their suitability with different antenna types. Section VIII provides a qualitative evaluation and comparison between all presented antenna designs in terms of gain, volume, bandwidth and reflection coefficient (S_{11}) according to their operating frequency bands. Section IX provides a critical analysis of the survey findings and an overview of the future trends for emerging CubeSat applications. The paper concludes with Section X.

II. PLANNAR ANTENNAS

Planar antennas such as patch and slot antennas are easy to fabricate, have low profile, low cost and easy to integrate with other Radio Frequency (RF) and microwave circuits [3]. These features make them ideal for CubeSats addressing most of the challenges and constraints of CubeSat. In addition, as compared to deployable antennas, i.e., helical and reflector antennas, planar antennas occupy smaller real estate and do not require deployment. This is important as it provides more

space on a CubeSat for solar cells and decreases the probability of deployment failure. Figs. 2 and 3 show examples of typical standard patch and slot antennas, respectively. They can be fed using different feeding techniques, i.e., microstrip line feed, coaxial probe feed, proximity coupled feed and aperture coupled feed. Tables 3 and 4 list the proposed planar antenna designs (e.g., patch and slot) for CubeSats and summarize their performance in terms of size, operating frequency, -10 dB bandwidth, gain, polarization, and reflection coefficient (S_{11}). We further discuss each proposed patch and slot antenna design in detail in section parts *A* and *B*.
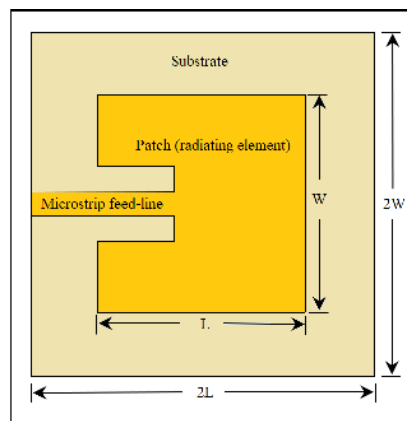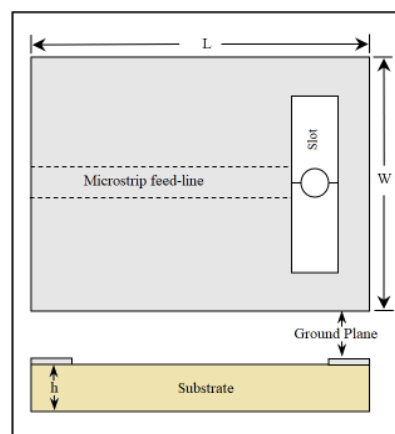

FIGURE 2. Standard patch antenna.

FIGURE 3. Standard slot antenna.

A. PATCH ANTENNAS

In this section, we have reviewed 18 patch antenna designs for CubeSats. These antennas operate in S, C, and X bands and provide a total gain ranging from 4.8 to 30.5 dBi. Amongst all patch antenna designs listed in Table 3, i.e., those in [11]–[28], the one in [15] and [16] have the smallest antenna physical size and hence they are suitable for use on 1U, 2U and 3U CubeSats. The design of [15] can also be implemented on the top of the solar cells because of its high transparency and hence allows for surface area reuse due to the integration of the antenna and solar cells. However, its main limitation is the resulting narrow bandwidth

TABLE 3. Proposed patch antenna designs for CubeSat.

Ref	Size ($\lambda_0 \times \lambda_0$)	Operating Frequency (GHz)	Bandwidth $|S_{11}| < -10$ dB (%)	Gain (dBi)	S_{11} (dB) at Center Frequency	CubeSat Type	Deployable	Polarization	Application
[11]	n/a	8.25 (X-band)	16.97	13	-40	1U	No	CP	Ground Communication
[12]	n/a	7.4 (X-band)	16.21	7.2	-13	1U	No	CP	Ground Communication
[13]	1.41×1.17	5.1 (C-band)	10.20	5.9	-17	1U	No	CP	Intersatellite Communication
[14]	0.78×0.78	2.45 (S-band)	44.90	8.22	- 45	3U	No	CP	Earth Observation
[15]	0.23×0.35	2.43 (S-band)	1.65	5.3	-14.5	1U, 2U, 3U	No	n/a	Ground Communication
[16]	0.19×0.20	2.45 (S-band)	2.45	4.8	-19	1U	No	CP	Ground/Intersatellite Communication
[17]	1.93×1.93	5.8 (C-band)	1.20	6.98	-21	1U	No	CP	Intersatellite Communication Educational
[18]	2.13×2.13	1st 8 (C-band) 2nd 11.2 (X-band)	1st 2.39 2nd 3.22	1st 6.45 2nd 5.34	1st -19 2nd -15.5	3U	No	Dual-CP	Ground Communication
[19]	0.82×0.82	2.45 (S-band)	45.75	8.5	-32.5	3U	No	LP	Ground Communication
[20]	1.2×1.2×2.4 deployable volume	3.6 (S-band)	n/a	30.5	n/a	6U	yes	LP	Ground Communication Remote Sensing
[21]	0.80×0.80	1.57 (L-band) 2.2 (S-band)	9.55 9.66	6 5.4	-27 -40	3U	No	CP	Ground Communication GPS
[22]	0.81×0.81	2.43 (S-band)	2.67	7.2	-16	1U	No	LP	n/a
[23]	3.33×3.33	10 (X-band)	40	15	-18	1U	No	CP	Remote Sensing
[24]	0.67×1.51	2.52 (S-band)	11.11	5.2	-23.5	3U	No	CP	Ground/Intersatellite Communication
[25]	0.70×0.70	2.45 (S-band)	32.6	9	-24	3U	No	RHCP	TT&C
[26]	0.75×0.75	2.25 (S-band)	11.11	4.87	-18.5	3U	No	CP	n/a
[27]	2.73×2.73	8.2 (X-band)	15.85	20.03	-15	1U, 2U, 3U	No	CP	High-speed Data Downlink
[28]	0.46×0.20	2.3 (S-band)	28.70	4.39	-40	1U	Yes	n/a	Ground Communication

TABLE 4. Proposed slot antenna designs for CubeSats.

Ref	Size ($\lambda_0 \times \lambda_0$)	Operating Frequency (GHz)	Bandwidth $|S_{11}| < -10$ dB (%)	Gain (dBi)	S_{11} (dB) at Center Frequency	CubeSat Type	Deployable	Polarization	Application
[34]	1.18×0.39	5.03 (C-band)	1.99	4.98	-17 dB	1U	No	LHCP	Intersatellite Communication
[35]	n/a	0.485/0.500 (UHF)	n/a	4	-29	1.5U	No	CP	TT&C
[36]	0.73×0.73	2.45 (S-band)	30.20	9.71	-21	3U	No	CP	Ground Communication
[37]	0.29×0.29	2.45 (S-band)	4.45	8.62	-30	2U	No	CP	Ground Communication
[38]	0.31×0.31	2.44 (S-band)	2.05	5.8	-34	1U	No	CP	Ground/Intersatellite Communication

(i.e., 1.65%) which leads to low data rate. On the other hand, the design in [23] provides a wide bandwidth of 40% with a high gain of 15 dBi at 10 GHz (X-band). In terms of gain, the proposed deployable S-band antenna design in [20] has reported the highest gain, i.e., 30.5 dBi as compared to all other S-band antenna designs listed in Table 3. However, its main limitation is the large deployable antenna size which makes it only suitable for 6U CubeSat.

Compared to C-band antenna designs in [13], [18], the C-band patch antenna design of [17], has the highest gain of 6.98 dBi at 5.8 GHz. However, its size, i.e., 100 mm × 100 mm, occupies a large space on CubeSat that otherwise could be used for solar cells. The X-band patch antenna design in [14], has the smallest reflection coefficient, i.e., −45 dB as compared to all patch antenna designs listed in Table 3.

In [11], Lehmensiek *et al.* proposed an X-band circularly polarized 2×2 shorted annular patches array for 1U CubeSat.

The key idea is to short circuit each single annular patch with the ground plane using six vias to achieve circular polarization (CP); see Fig. 4 (a). Moreover, as shown in Fig. 4 (b), the array elements are fed using a ring resonator at the middle of the array which is connected to all four patches via strips. The proposed shorted annular patches array is fed using a sequential phase feeding network. It achieves a small reflection coefficient of -25 dB at 8.25 GHz with a wide bandwidth of 16.97% (7.5 – 8.9 GHz) and a total gain of 13 dBi at 8.25 GHz, respectively. The authors reported only simulation results.
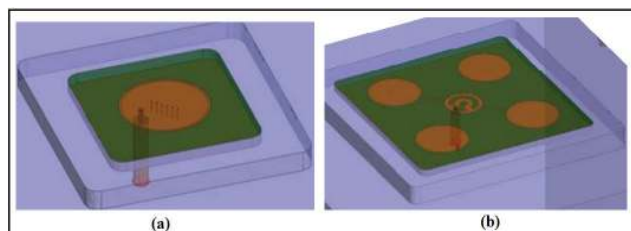
FIGURE 4. Shorted patches antenna model on 1U CubeSat: (a) single element and (b) 2×2 array elements [11].

Coll [12] presented a rectangular aperture coupled stacked patch antenna for CubeSat [12]; see Fig. 5 (a). As shown in Fig. 5 (b) (layer no. 3), to enhance the bandwidth and achieve a good circular polarization, the author used a crossed 45° shift slots to excite the two orthogonal elements with a 45° phase shift. The proposed X-band antenna design is fed by a microstrip line via crossed slot in the ground plane. The lengths of the two crossed slots have a significant effect on the bandwidth, the axial ratio, and the radiation pattern. The proposed antenna achieved a total measured gain of about 7.2 dBi at 7.4 GHz, measured wide bandwidth, i.e., 16.21% (7.3 – 8.5 GHz) and measured high reflection coefficient of -13 dB at 7.4 GHz. Its main limitation, however, is the high reflection coefficient which means more power is reflected back to the source instead of being transmitted into space.

Recently, designs of patch antenna arrays which consist of many sub-array elements and are fed by different feeding networks are proposed to enhance the antenna gain and to electronically steer the antenna's radiation beam. This is important as it maintains the communication link during the CubeSat's maneuver. The challenge is how to achieve a superior gain by implementing small patch antenna arrays on limited space on CubeSat. In [13], Maged *et al.* proposed a design of four antenna array elements for CubeSat cross-link communications. As shown in Fig. 6 (a) and (b), each array element consists of two 14 mm $\times$ 14 mm transparent patch antennas and is implemented on each face of 1U CubeSat. The main idea is to implement two square patches on a glass substrate to achieve transparency and hence allow the sunlight to reach the solar cell behind the antenna through the glass. Moreover, to achieve circular polarization, each patch
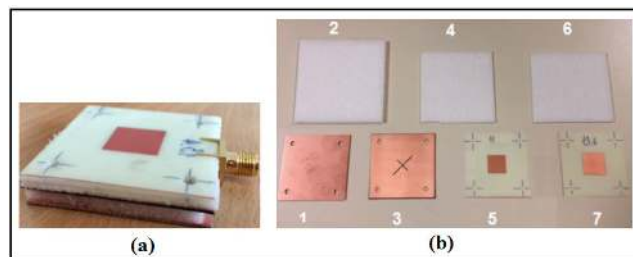

FIGURE 5. Proposed antenna, (a) stacked patch and (b) layers including the cross slots (no. 3) [12].
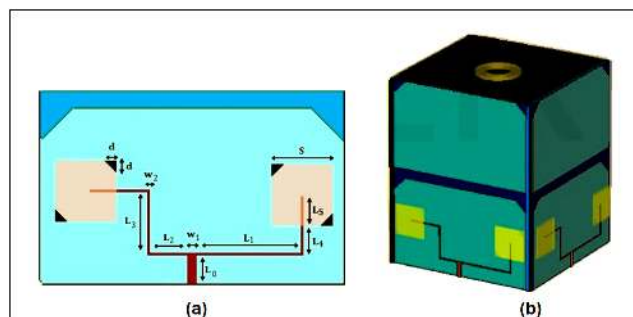

FIGURE 6. Proposed antenna: (a) Individual 1 $\times$ 2 array element, and (b) 4 array elements on 1U CubeSat [13].

is truncated from the two sides. The authors proposed implementing four 1×2 patch antenna arrays on four CubeSat faces and using the T-junction power divider to feed them with sequential phase rotation. Each proposed 1×2 patch antenna array element has a total volume of 83mm $\times$ 69mm $\times$ 1mm. It achieves a simulated reflection coefficient of -17 dB at 5.15 GHz (with solar cell) with a wide bandwidth of 10.20% (4.78 – 5.3 GHz), and -21.5 dB at 5.1 GHz (without solar cells) with a bandwidth of 8.43% (4.87 – 5.3 GHz). Moreover, the proposed antenna provides a total gain of 5.9 dBi (with solar cells) and 8 dBi (without solar cells) at an operating frequency of 5 GHz. We see that the use of solar cells influences the antenna's performance. The authors observed a decrease of the gain from 8 to 5.9 dBi and an increase of the reflection coefficient from -21.5 to -17 dB when the antenna is placed above the solar cells. This is because practical solar cells have a conductivity of about 103 (S/m) which leads to a reduction of 2-3 dBi in the gain for antennas that operate in the 1-10 GHz band [29]. Compared to C-band planar antenna designs presented in [17], [18], the C-band patch antenna in [13] has a wider bandwidth.

In [14], Nascetti *et al.* proposed a high gain four element patch antenna array for 3U Tigrisat CubeSat. The antenna is proposed to be mounted on one face (100mm $\times$ 100 mm) of 3U CubeSat and used for Earth Observation applications. The main idea is to increase the antenna's gain and achieve CP by making each sub-array of the two adjacent patches orthogonally oriented (90°) and feed them using a Wilkinson power divider; see Fig. 8 (a) and (b). This also leads to an increase in the signal strength and isolation between the power ports achieving very good input impedance matching.
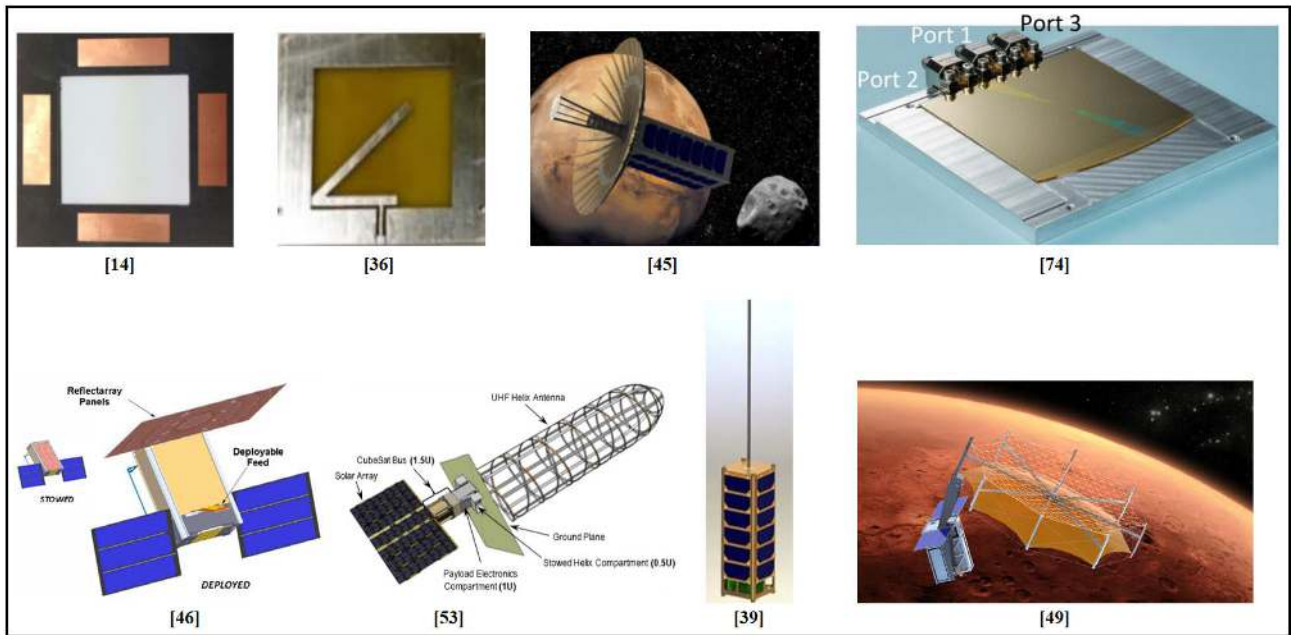
FIGURE 7. Examples of different types of proposed antenna designs for CubeSat.

The proposed antenna has a simulated high gain of 8.22 dBi and a small reflection coefficient of −45 dB at 2.45 GHz with a wide bandwidth of 44.9% (2.05-3.15 GHz). The total size of the proposed antenna is 96 mm × 96 mm with an area of 57mm × 57mm left in the middle for camera optics; see Fig. 8. Compared to the designs in [15], [21], [22], the design of [14], achieves higher gain at a similar operating frequency band, i.e., S-band. Moreover, the proposed antenna has a wider −10 dB bandwidth as compared to all patch and slot antennas reported in [15], [18], [21], [22]. Its main limitation, however, is that the authors have not considered or presented tests of the interference that could occur between the proposed antenna and camera optics as they are implemented next to each other.

The authors of [15], designed a transparent mesh patch antenna for 3U CubeSat communication with ground station. As shown in Fig. 9, the key idea is to use transparent substrate (quartz material) with a 43.7mm² square meshed lines implemented on an 80.1 mm² square ground plane. The main challenge for designing such an antenna was that the relationship between the thickness of the copper lines of the mesh and the antenna performance is not linear. This means decreasing the thickness of the copper lines leads to a decrease in the radiation efficiency and gain. The optimal obtained line thickness that provides 90% transparency, bandwidth of 1.65%, efficiency of 85.9%, reflection coefficient of −14.5 dB and a total antenna gain of 5.3 dBi at 2.43 GHz was 0.1 mm with a total mesh size of 28.44mm × 43.7mm. The main advantage of the proposed design is its high transparency and hence it is proposed to be placed above the solar cells allowing the sunlight to reach the solar cells. This will effectively reduce the occupied area by half as the antenna and the solar
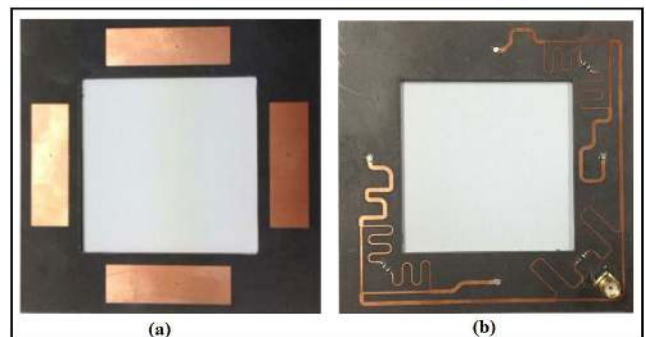

FIGURE 8. Proposed patch antenna array: (a) top view (radiators) and (b) bottom view (feeding network) [14].

panels will share the same area. However, at low frequency (less than 2.4 GHz), it achieves poor transparency.

In [16] Podilchak *et al.* presented the design of a CP meshed patch antenna for small satellites including 1U CubeSat, see Fig. 10. The proposed antenna has a small total size of 24.1mm × 24. 8mm, operates at 2.45 GHz (S-band) and is fully integrated with a solar cell. To achieve CP, the proposed antenna is excited by two orthogonal ports and the feed network is integrated underneath the solar cell. This enhances the bandwidth and improves the antenna's total gain. Moreover, the meshed lines of the proposed antenna are placed above glass to provide high transparency and hence sunlight can reach the solar cells. This is important as it provides more space for solar cells and hence more power budget for the subsystems. The authors reported simulated and measured reflection coefficients and bandwidths at 2.385 GHz of −18 dB (BW = 1.35%) and −19 dB (BW = 2.45%) respectively. In addition, the proposed antenna achieved similar simulated
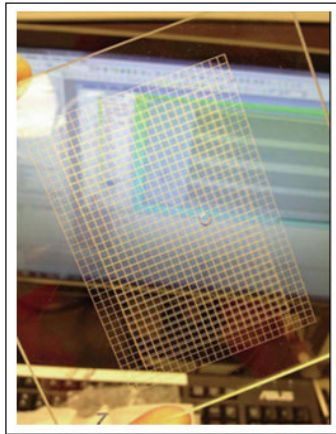
FIGURE 9. Proposed transparent mesh patch antenna for 3U CubeSat [15].

FIGURE 11. Square antenna array: (a) Individual element of 2 × 2 sub-array and (b) with nine identical elements (3 × 3) [17].
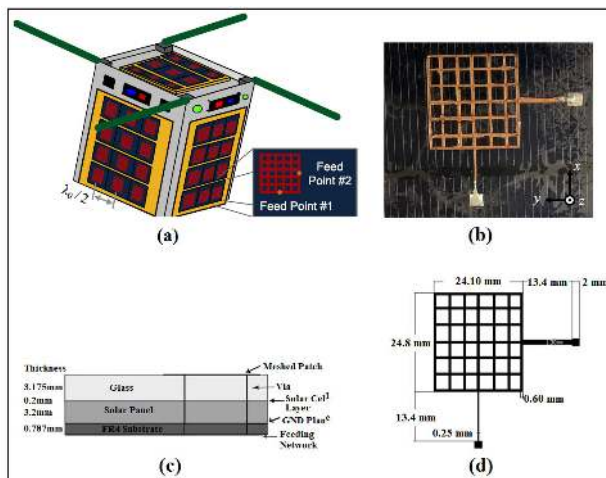

FIGURE 10. Proposed patch antenna design, (a) mounted on 1U CubeSat's module, (b) manufactured, (c) top view and (d) cross section view [16].

and measured gains of about 4.8 dBi at 2.45 GHz. The authors claim that the proposed antenna can be used to implement phased arrays system because its structure is compact, and it has a small size; see Fig. 10 (d). This is important as it can significantly improve the total gain and provides long distance communications. Its main limitation, however, is its narrow bandwidth, i.e. 2.45%.

Another design that uses a patch antenna array on one face of 1U CubeSat for intersatellite communications is presented in [17]. As shown in Fig. 11 (b), 3 × 3 nine identical sub-array elements are implemented on 1U CubeSat's face. Each sub-array element consists of 2 × 2 individual rectangular patch elements and are fed sequentially; see Fig. 11 (a). To achieve CP, every two elements of 2 × 2 sub-array are implemented orthogonal to each other. The antenna array operates at 5.8 GHz and achieves a small, measured reflection coefficient of −21 dB, simulated total gain of 6.98 dBi and a narrow bandwidth of 1.20%. The main advantage of the proposed design is its ability to steer the beam by feeding the subarray at different angles, i.e., 0°, 90°, 180°, and 270° and hence establish a good communication link between
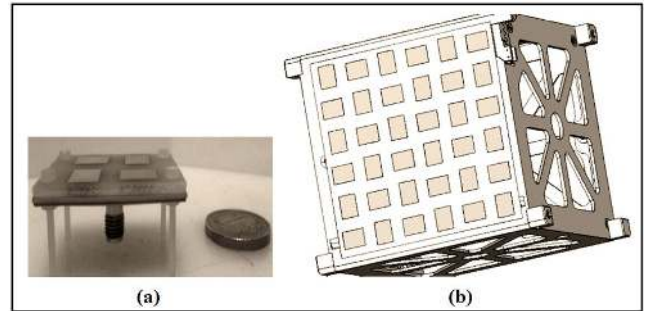
CubeSats and ground stations duringmaneuvering. In addition, compared to the antenna designs presented in [14], [21], the patch antenna array design reported in [17], is the only design that has the ability to steer the beam. This is important as it has the ability to provide a continuous communication link with a ground station.

The authors of [18], presented a transparent dual-band patch antenna array that operates at two operating frequencies of 8 GHz and 11.2 GHz for 3U CubeSat. The key idea is to implement a transparent patch on a glass substrate that can be placed above the solar cells and hence provide more space for solar cells; see Fig. 12 (a). The sunlight can reach the solar cells because of transparency of the proposed antenna design. The 8mm × 8mm top patch layer is used for an operating frequency of 11.2 GHz and is fed via two probes from a coupler at the bottom layer. There is also a 6.3mm × 6.3mm patch under the top patch layer which was used to obtain an operating frequency of 8 GHz and it is fed from the top patch layer. Moreover, the dual band coupler is used to produce two input with a 90° phase shift to the antenna array. This leads to right and left hand circular polarization (RHCP and LHCP). In addition, as shown in Fig. 12 (b), nine of the proposed transparent antennas are integrated in a 3 × 3 array with a total size of 80mm × 80mm. They reported total gains of 6.45 and 5.34 dBi at 8 GHz and 11.2 GHz, respectively. Moreover, the proposed antenna achieved a −10 dB bandwidths of 2.39% at 8 GHz and 3.22% at 11.2 GHz. However, the main limitation of the proposed antenna is its high reflection coefficients, i.e., −19 dB at 8 GHz and
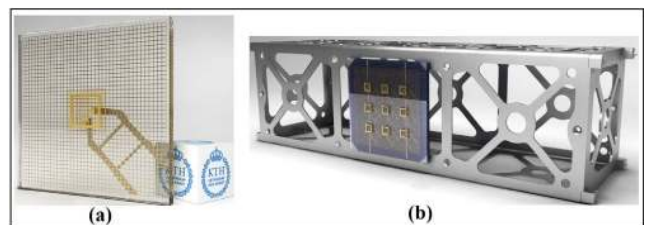

FIGURE 12. Transparent patch antenna: (a) single element and (b) 3 × 3 array elements on 3U CubeSat [18].

−15.5 dB at 11.2 GHz. This means more power is reflected instead of being radiated into space.

Shorting walls and shorting pins are techniques that are used to reduce the antenna size without affecting its performance; i.e., gain, bandwidth and impedance matching [30]. In [19], Abulgasem *et al.* proposed a high gain F-shaped patch antenna that operates at 2.45 GHz (s-band) with a total size of 100mm × 100mm for a 3U CubeSat. The main idea is the use of three shorting pins between the radiating patch element and the ground plane to reduce the antenna physical size by increasing the effective electrical length of the radiating patch; see Fig. 13. Moreover, to increase the bandwidth of the proposed antenna, the authors used two arms on the upper patch with different lengths. This generates two resonant frequencies and hence increases the bandwidth. They reported a wide bandwidth of 45.75%, small reflection coefficient, i.e. −32.5 dB and high gain of 8.5 dBi at operating frequency 2.45 GHz. The proposed F-shaped patch antenna has the highest gain and largest bandwidth as compared to other patch antenna designs reported in [15], [21], [22]. However, the proposed antenna is not robust because of the used shorting pins between the upper patch and ground plane.
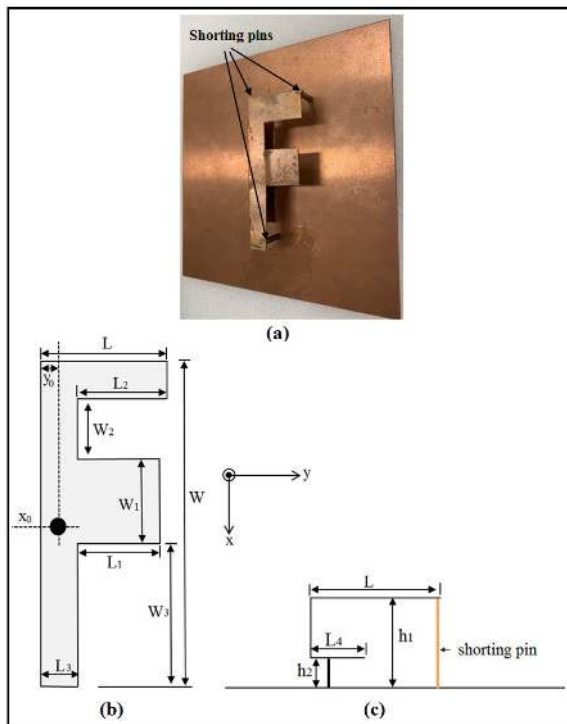

FIGURE 13. F-shaped patch antenna, (a) fabricated, (b) top view and (c) side view [19].

The authors of [20], proposed a large, deployable 16 × 16 patch array for a 6U CubeSat; see Fig. 14 for remote sensing applications. The proposed antenna design has two tensioned membranes that are folded into a 2U payload size with four deployable boom structures and operates at 3.6 GHz (S-band). The main advantage of this proposed antenna is that the antenna occupies a small size when it is folded and

FIGURE 14. S-band deployable patch antenna array for 6U CubeSat [20].

hence provides more space for solar cells and payload on a 6U CubeSat. The large patch antenna array deploys when the CubeSat is in orbit to establish a communication link with the ground station. The authors reported a superior gain of 30.5 dBi; however, its main drawback is the use of a complex deployment mechanism which may lead to a mission failure if the antenna does not deploy.

The authors of [21], propose a dual-band Circularly Polarized (CP) patch antenna for 3U CubeSat. As shown in Fig. 15 (a), the antenna design is proposed to be implemented on one face (100mm × 100 mm) of 3U CubeSat for communication with ground station and to operate at two different operating frequencies, i.e., 1.57 GHz (L-band) and 2.2GHz (S-band). As shown in Fig. 16 (a), the patch antenna design consists of a lower band (1.57 GHz) on the top layer which acts as Global Positioning System (GPS) antenna to receive positioning signals from GPS satellites
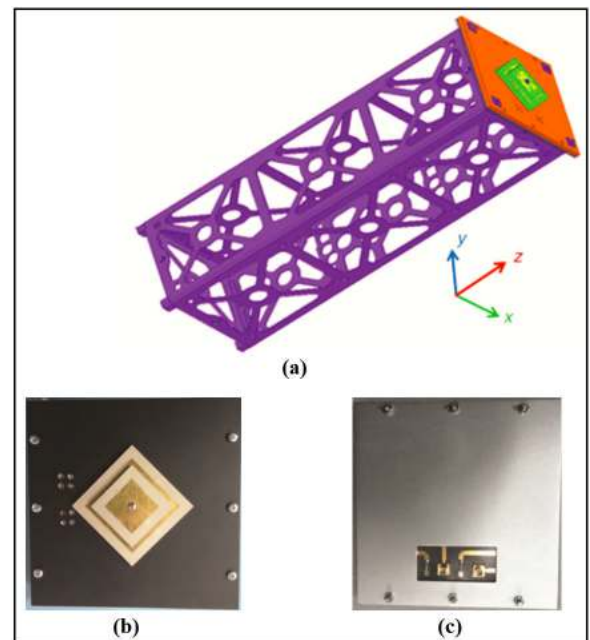

FIGURE 15. Dual band stacked patch antenna for CubeSat: (a) mounted on 3U CubeSat, (b) top view and (c) bottom view [21].

and an upper band (2.2 GHz) in the middle layer which works as a transponder to transmit data to ground station. The main idea is the use of dual-feed technique to feed the lower and upper band antennas using 3-dB hybrid couplers; see Fig. 15 (b). This is important as it reduces the number of antennas on CubeSat and hence reduces interference between these antennas and other electronic components. It also provides sufficient real estate to mount solar cells. The authors reported total measured gains of 6 and 5.4 dBi for the upper and lower bands respectively; see Fig. 16 (b) and (c). Moreover, Fig. 16 (a) shows the measured reflection coefficient of −27 dB with bandwidth of 9.55% for lower band and −40 dB with bandwidth of 9.66% for upper band. The proposed patch antenna exhibits a good performance at two operating frequencies, i.e., 1.57 and 2.2 GHz. However, its main limitation is the large ground plane, i.e., 110mm × 110mm, which is larger than the CubeSat face (100mm × 100mm). Another limitation is that the proposed antenna is unable to electronically steer its radiation beam to re-establish the communication link with ground station during CubeSat maneuver.
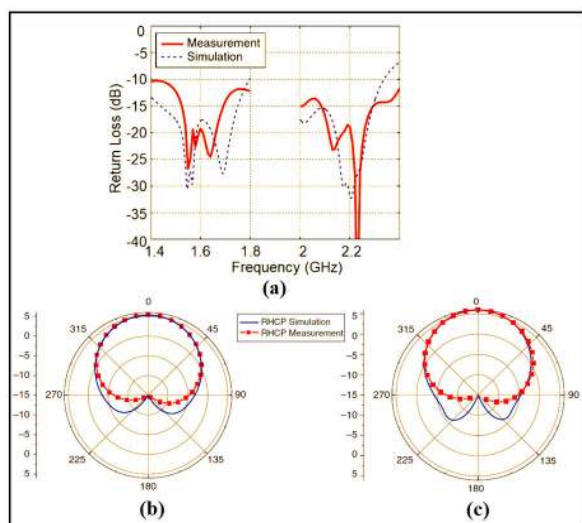

FIGURE 16. Results of proposed antenna: (a) reflection coefficient, (b) radiation pattern at 1.57 GHz and (c) Radiation pattern at 2.2 GHz [21].

Another transparent mesh patch antenna design is presented in [22]. The authors proposed a new technique of using three transparent meshed patch configurations on CubeSat's surface to enhance the bandwidth. As shown in Fig. 17, the antenna is comprised of three elements utilizing the same feedline. Moreover, the proposed antenna has a high transparency of about 70% and hence it can be laid on the top of solar cells. The total size of the proposed meshed patch antenna is 100mm × 100mm and the side lengths of its three elements are 30, 30.2 and 30.4mm, respectively. The proposed antenna with three meshed patch elements provides a measured −10 dB bandwidth of about 2.67% (2.413 − 2.478), reflection coefficient of −16 dB and total gain of 7.2 dBi at 2.43 GHz.
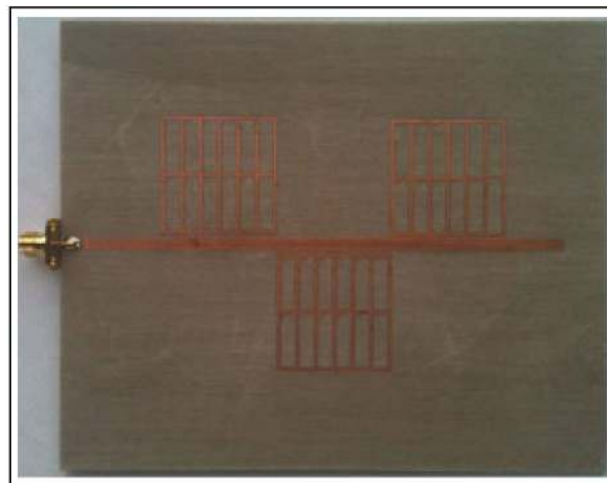

FIGURE 17. Triple element meshed patch antenna [22].

In [23], Sarbakhsh *et al.* presented a multifunctional, high gain and CP transparent subarray patch antenna for CubeSat remote sensing applications. The antenna operates in the X-band and has a total size of 10 mm × 10 mm. As shown in Fig. 18 (a) and (b), the proposed 2 × 2 subarray antenna contains two layers with a cross slot being etched on the bottom ground plane. To achieve CP and enhance the antenna performance, the authors used the fabry-perot cavity approach [31], [32] and a parallel sequential rotation feeding network technique, see Fig. 18 (c). The sequential feeding network is an unequal power divider and has four output 50 Ω ports with 90° phase delay between ports in anticlockwise direction. In addition, they used a combination of Indium Tin Oxide (ITO) and Copper (Cu) coating layers on transparent polyethylene terephthalate (PET-G) substrate. These materials provide high transparency and good conductivity. Therefore, the solar panel is placed between TMM10i and PET-G substrates, see Fig. 18 (d). This is important as it provides more space for solar cells on CubeSats and hence better energy harvesting. They reported simulated and measured reflection coefficients of −25 and −18 dB at 10 GHz with a wide −10 dB bandwidth of 40% (8-12 GHz), respectively and a high measured gain 15 dB at 10 GHz with solar cell.

The authors of [24], presented a circular polarized microstrip antenna for both ground and intersatellite communications. The proposed antenna operates in the S-band (2.34 − 2.62 GHz) and has a total size of 80mm × 180mm; see Fig. 19 (a) and (b). To achieve LHCP or RHCP with good antenna performance, the authors used a closed loop travelling wave as a radiating element which was fed by a hybrid coupler that has two ports; see Fig. 19 (a). The antenna is fed via ports 1 and 2 by same magnitude but difference phase. For example, when feeding the antennas via ports 1 and 2 with same magnitude but a quadrature phase difference of −90°, RHCP is obtained while the LHCP is obtained by feeding those two ports with phased difference of +90°. The antenna has a simulated reflection coefficient of −27 dB at 2.43 GHz with bandwidth of 16.05% and measured
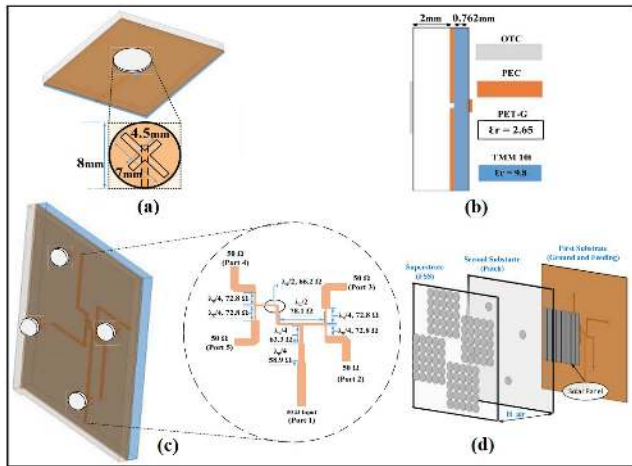
FIGURE 18. Geometry of Proposed antenna: (a) single antenna element, (b) side view, (c) 2 × 2 subarrays with feeding network [23].
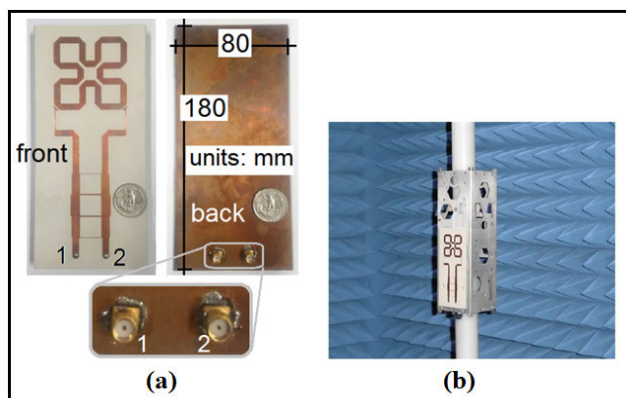

FIGURE 19. Proposed antenna, (a) fabricated and (b) mounted on 3U CubeSat during measurements [24].

reflection coefficient of −23.5 at 2.52 GHz with a measured bandwidth of 11.11%. The simulated and measured gains at 2.45 GHz are 7 and 5.2 dBi respectively.

Fig. 20 shows a wideband low profile stacked-patch antenna for 3U CubeSat communication design that was designed and presented by Veljovic and Skrivervik [25]. The proposed antenna operates in the S-band (2-2.45 GHz), has a total size of 100mm × 100mm and uses an aperture-coupled stripline feed structure technique, see Fig. 20. To enhance the performance of the proposed antenna, the authors enclosed the asymmetric-stripline feeding network with metallic walls. This is important as the obtained cavity improves the electric field and boosts the coupling between the radiating element (patch) and feeding structure through near electromagnetic field. Hence, the antenna's gain increases as the back lobe is redirected forward improving its radiation performance. Fig 20 (b) shows the layers of the proposed antenna including the use of Wilkinson power dividers and phase-delay lines for the feeding network which prevents the signal reflection and enhance the cross-polarization. Fig. 20 (a) and (c) shows the proposed antenna mounted on the 3U CubeSat mock-up and the crossed coupling slot
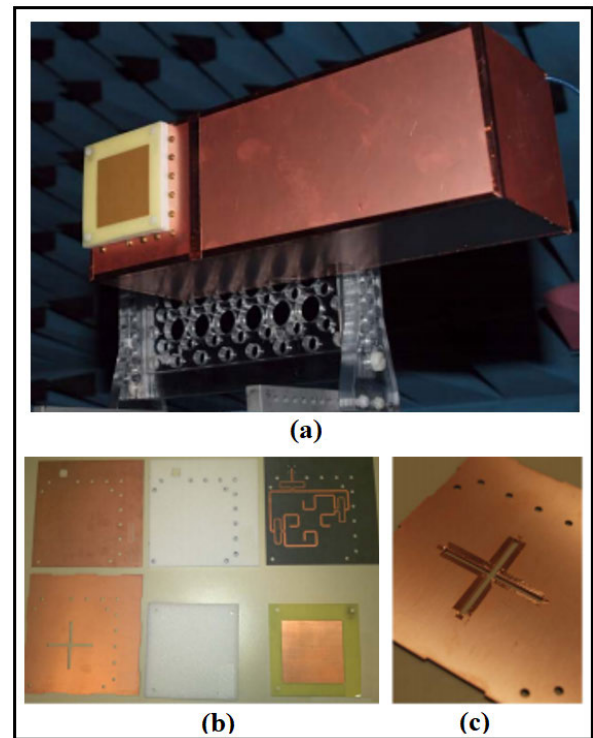

FIGURE 20. Proposed patch antenna design, (a) Antenna's layers, (b)Coupling slot and (c) Antenna mounted on 3U CubeSat's body [25].

covered with the conductive tape, respectively. The authors reported a measured reflection coefficient of −24 dB at 2.12 GHz and −22 dB at 2.48 GHz with a wide bandwidth of 32.6% ranging from 1.80 GHz to 2.60 GHz. The proposed antenna achieved a measured gain of 9 dBi at 2.45 GHz.

In [26], Ygnacio-Espinoza *et al.* proposed a quasi-transparent meshed and circularly polarized patch antenna for S-band CubeSat applications. The proposed antenna operates at 2.25 GHz (S-band) and has a total size of 100mm × 100mm, see Fig. 21 (a). The key idea is to integrate the proposed patch antenna into the solar cells using the cover glass and solar cell as a substrate; see Fig 21 (b). Moreover, to increase the bandwidth and enhance the antenna performance, the authors used the metamaterial with Reactive Impedance Surface (RIS) as the ground plane for the proposed circular patch antenna. The authors reported a simulated reflection coefficient of −18.5 dB with −10 dB bandwidth of 11.11% (2.20-2.45 GHz) and a 3D total gain of 4.87 dBi at 2.25 GHz. Compared to other S-band antenna designs in [15], [21], [22], the proposed antenna in [26], has wider −10 dB bandwidth. However, it has lower gain compared to the mentioned studies.

In [27], Ta *et al*, presents a high gain X-band patch array antenna for small satellites including CubeSats to achieve high aperture efficiency and low side lobe CP. As shown in Fig. 22, the proposed antenna has a total size of 100mm × 100mm and operates in 7.52 − 8.82 GHz band. Its 4 × 4 patch array consists of 16 CP stacked patch elements. This is important as it leads to high aperture efficiency.
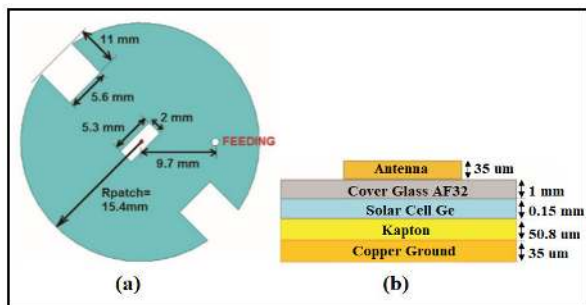
FIGURE 21. Proposed patch antenna, (a) geometry, and
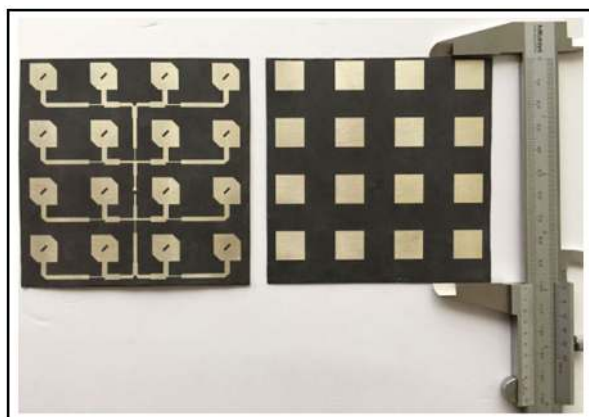(b) Cross-sectional view of antenna integrated with solar cells [26].

FIGURE 22. Fabricated proposed array antenna [27].

The other approach the author used to achieve low side lobe levels is to feed the antenna via unequal 1-16 series parallel power dividers. Moreover, each driven patch element of the 16 patch elements, has a slot and two truncated corners to achieve CP radiation, see Fig. 22. The proposed antenna achieved a measured reflection coefficient of −15 and −12 dB at 7.7 and 8.6 GHz respectively. It provides a measured −10 dB bandwidth of 15.85%, high gain of about 20.03 dBi, low sidelobe level of −20 dB and an aperture efficiency of 86.5%.

The main limitation of existing planar antenna designs that operate in S-band frequency, i.e., 2-4 GHz, is their large size [33]. To reduce the planar antenna size without affecting the operating frequency, the authors of [28] introduced a deployable microstrip patch antenna with the fractal structure for 1U CubeSat. As shown in Fig. 23 (a), the key idea is the use of Koch snowflake fractal structure which leads to miniaturization of the antenna's size while at the same time yielding high gain and small reflection coefficient, large bandwidth and good impedance matching. The authors proposed a simple deployment of the fractal antenna; see Fig. 23 (b). The proposed antenna has a small reflection coefficient of −28 dB at 2.3 GHz and a wide bandwidth of 28.7%. It also provides a small gain of 4.39 dBi at 2.3 GHz. The main advantage of the proposed antenna is its small size, i.e., 60 mm × 26.3 mm × 0.02mm. Its main limitation, however, is its omnidirectional pattern that results in low gain.
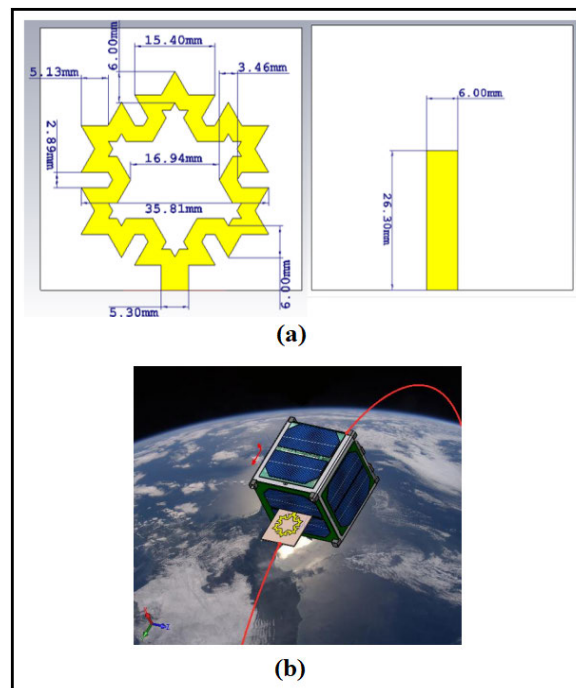

FIGURE 23. The proposed fractal antenna (a), (b geometry and
(b) deployed on CubeSat [28].

B. SLOT ANTENNAS

Slot antennas usually consist of metal flat surfaces (plates) with one or more holes (slots) and operate in frequencies ranging from 0.3 to 25 GHz. Proposed slot antenna designs for CubeSats are very limited because they provide linear polarization and have low directivity which results in weak signal strength and low gain. To address the aforementioned limitations, different approaches and techniques were proposed and used; see Table 4. Amongst all these slot antenna designs, i.e., those in [34]–[38], the antenna design of [36], has the highest gain of 9.71 dBi and widest −10 dB bandwidth, i.e., 30.2%. However, its main limitation is its large size. On other hand, the CPW-fed slot antenna presented in [37], has the smallest size as compared to all other slot antenna designs listed in Table 4. This is important as it provides more space for solar cells integration, e.g., more power can be generated on board the CubeSat.

The authors in [34], proposed the design of a CP slot antenna array for crosslink CubeSat communications. Fig. 24 (a) shows a single slot antenna array element which consists of four slots with a total size of 70.5mm × 23.5mm and operates in C-band. They used a Substrate Integrated Waveguide with four slots on the top copper layer to achieve low loss and good radiation performance. The main idea is to place two SIW slot antenna array elements behind the CubeSat's wall on each CubeSat's face leaving sufficient area to mount solar cells or other components; see Fig. 24 (b). The CP is achieved by using a quadrature hybrid coupler in the feeding network providing equal magnitude of power through ports and 90° phase difference between the slot array elements. Moreover, a control switch circuit is also used to steer
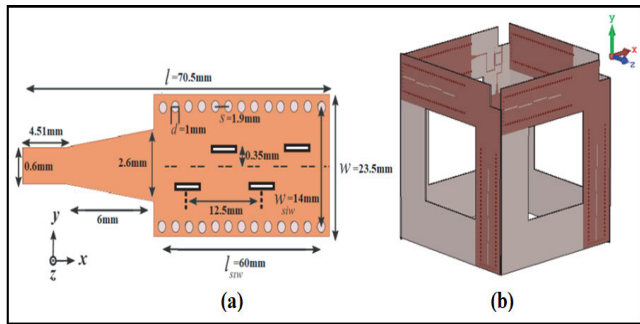
FIGURE 24. Slot antenna array: (a) geometry of individual array element and (b) slot array elements on four CubeSat's surfaces [34].

FIGURE 25. Slot antenna for 1.5U CubeSat: (a) with Solar Panels and (b) feeding network [35].

FIGURE 26. Proposed fabricated CPW-fed slot antenna with MSS: (a) geometry, and (b) on a 3U CubeSat model [36].

the beam into different directions. This is important as it saves power scanning the beam in the desired direction allowing for a reliable link even when re-orienting the CubeSat. The authors reported simulated and measured gains of 5.08 dBi and 4.98 dBi at 5GHz, respectively. The proposed antenna has a measured reflection coefficient of −17 dB at 5.03 GHz with a measured narrow bandwidth of 1.99%. The proposed antenna provides beam steerability. Compared to the designs in [36], [37], the antenna design presented in [34], has larger antenna size and smaller gain.

In [35], Tarig and Baktur proposed a cavity backed slot antenna design for uplink at 485 MHz (UHF) and downlink at 500 MHz (UHF) CubeSat communications. As shown in Fig. 25 (a), a loop meander-line slot is wrapped and mounted all around the four faces of a 1.5U CubeSat and between solar cells. Then every two adjacent parts of the loop are fed with a phase difference of 90° to obtain CP; see Fig. 25 (b). This is important as it ensures that the communication link is established regardless of CubeSat's orientation. The frequency of the proposed slot antenna can be tuned for uplink or downlink communication by adjusting the length of the meander portions. The proposed slot antenna design achieved a total gain of 4 dBi at UHF band (485 and 500 MHz), reflection coefficient of about −28 and −29 dB for uplink and downlink, respectively. However, its main limitation is its low gain.

In [36], Tubbal *et al.* has presented another S-band CPW-fed slot antenna design for 3U CubeSat. The key idea is to design and use Metasurface Substrate Structure (MSS) above the radiating slot to redirect the back-lobe radiation pattern forward; see Fig. 26. This is important as it significantly increases the total gain in the boresight direction (z-direction) and reduces the interference with the components inside the 3U CubeSat. The antenna has a total physical size of 90mm × 90mm × 10.5mm. The proposed antenna provides simulated and measured gains of 9.71 and 8.8 dBi respectively. It also has a small reflection coefficient of −21 dB with a wide bandwidth of 30.20% at an operating frequency of 2.45 GHz. Its main limitation, however, is its large profile with a height of about 10.5mm. This can be an issue during the vibration and the deployment stage. Compared to [37], which uses part of the CubeSat's body as cavity reflector, the use
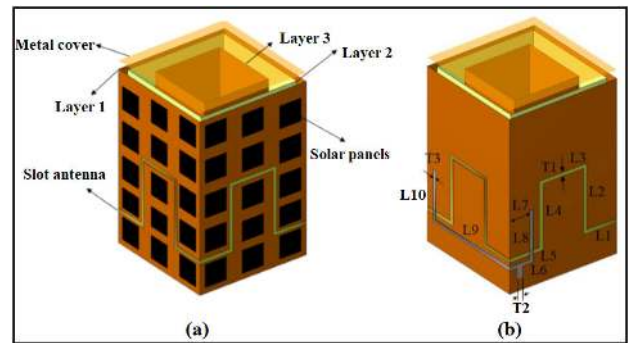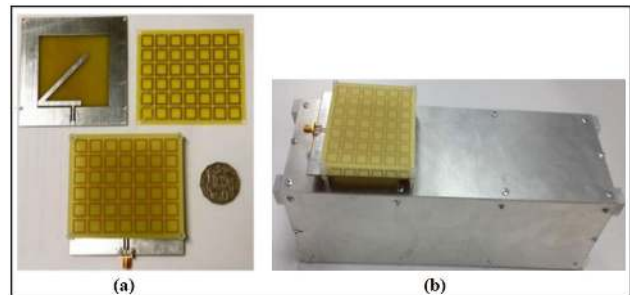
of MSS in [36], provides higher gain and does not affect the mechanical structure of CubeSat as it is placed above the CubeSat's surface. In terms of size and reflection coefficient, the design of [37], has smaller size and reflection coefficient as compared to the design presented in [36].

The cavity approach is an important technique to increase the antenna's total gain by suppressing the unwanted back lobe radiation redirecting it boresight direction. In [37], Tubbal *et al.* presented a CPW-fed high gain slot antenna design that operates at 2.45 GHz for 2U CubeSat communication. As shown in Fig. 27 (b), the authors proposed the use of part of the CubeSat face, i.e., (100mm × 200mm) at the back of the antenna as a cavity to redirect the back-lobe radiation pattern forward and hence increase the antenna total gain. This is significant as it provides long distance communication, higher data rate and reduces the interference with the electronics inside the CubeSat. The authors also used the lightening shape feedline with 45° phase angles between the horizontal and slanted (S) feed sections to achieve circular polarization; see Fig. 27 (a). The proposed antenna has a total size of 36mm × 36mm which occupies only 12.96% of one face of 1U CubeSat. The authors reported a small reflection coefficient of −30 dB with bandwidth of 4.45% and a gain of 8.62 dBi (unidirectional pattern) at 2.45 GHz. However, the main limitation of the proposed antenna design is that shifting down part of the CubeSat's body to form cavity can significantly affect the mechanical structure of the CubeSat and reduce the available surface area for the electronic components inside the CubeSat. Another limitation

TABLE 5. Proposed dipole, monopole and Yagi-Uda antenna designs for CubeSats.

| Ref	Size ($\lambda_0 \times \lambda_0$)	Operating Frequency (GHz)	Bandwidth $\|S_{11}\| < -10$ dB (%)	Gain (dBi)	S_{11} (dB) at Center Frequency	CubeSat Type	Deployable	Polarization	Application
[39]	0.26 (long)	1st 0.146 (VHF) 2nd 0.438 (UHF)	1st 13.70 2nd 6.85	1st 2.06 2nd 3.35	1st -18.5 2nd -21	3U	yes	LP	Ground Communication
[40]	Printed dipole 0.66×0.66	2.5 (S-band)	4.8	5.03	-27.35	1U	no	LP	Intersatellite Communication
[41]	Printed dipole 0.45×0.45	2.45 (S-band)	33.46	3.49	-27.5	1U	no	CP	Ground Communication
[42]	Dipole 1.42 (long) Monopole 0.45 (long)	Dipole 0.144 (VHF), 0.435 (UHF) Monopole 0.144 (VHF), 0.435 (UHF)	Dipole 8.68 5 Monopole 4.86 5.98	Dipole 2.59 3.91 Monopole 2.14 4.35	Dipole -14.5 -15 Monopole -35 -42	1U	yes	CP	Ground Communication
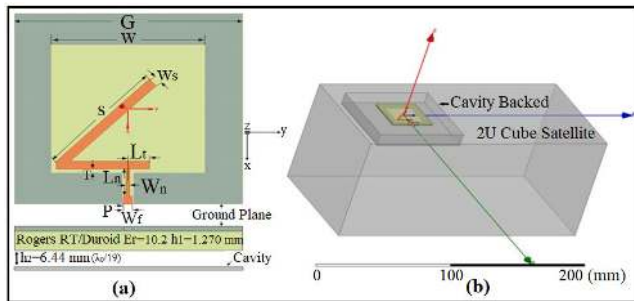
FIGURE 27. Slot antenna: (a) configuration of slot antenna, and (b) on a 2U CubeSat [37].

is the possibility of losing communication with ground station during the maneuvering of the CubeSat as only one antenna on one face is present.

The authors of [38], presented a low profile cavity backed crossed slot antenna for communication between CubeSats and ground stations as well as intersatellite links. The key idea is to use the cavity backed tapered crossed slot with a combined probe feed; see Fig. 28. This is important as it enhances the impedance bandwidth. Moreover, orthogonal crossed slots with slightly different lengths and 45° phase shift in the x and y axis are used to achieve CP and hence enhance signal reception. This is important as it helps in establishing cross link communication between CubeSats, especially during maneuvering. The proposed antenna has a low reflection coefficient of −34 dB (measured) and −38 dB (simulated) and provides a total measured RHCP gain of 5.8 dBi at an operating frequency of 2.44 GHz. It also achieved a −10-dB bandwidth of 2.05% (2412 – 2462 MHz). The proposed crossed slot antenna design has a small physical size, i.e., 38mm × 38mm. however, its main limitation is its narrow bandwidth. In terms of gain, the designs in [36], [37] provide higher gain than the proposed antenna design in [38]. The main limitations of all designs reported in [36]–[38], is the
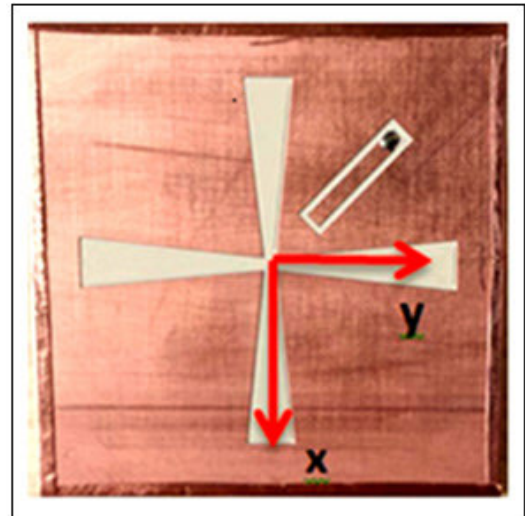
FIGURE 28. Cavity backed crossed slot antenna [38].

possibility of losing communication link with the ground station and other CubeSats during the reorientation of the CubeSat. This is because the antenna designs are proposed to be placed on only on face of CubeSat and their beam are not steerable.

III. DIPOLE AND MONOPOLE ANTENNAS

Dipole and Monopole antennas are the simplest and well understood designs. In this section, the performance of four dipole and monopole antenna designs, i.e., those in [39]–[42], for CubeSats are reviewed in terms of their total gains, size, bandwidth, reflection coefficient and deployment mechanism. As set out in Table 5, these dipole antenna designs operate at the Very High Frequency band (VHF) and S-band. They achieve gains ranging from 2.06 to 5.03 dBi. The printed S-band dipole antennas of [40], [41], have high gain, wide bandwidth and smaller reflection coefficient as

compared to deployable dipole antenna designs in [39], [42]. Moreover, the monopole design in [42] achieves the smallest reflection coefficient of −35 and −42 dB at 144 and 435 MHz respectively; however, its bandwidth is very narrow, i.e., 4.86% for VHF and 5.98% for UHF.

The use of more than one antenna for different functions on the CubeSat such as telemetry and telecommands, occupies more space and increases the interferences between the antennas and the electronic components [43]. To reduce the number of antennas used for the CubeSat, the authors of [39], proposed a dual band single monopole antenna that operates at 146 MHz (VHF) and 438 MHz (UHF) to transmit and receive data simultaneously. The main idea is to use a diplexer for the transmission and reception of data with a single antenna. As a result, the antenna can be used for both uplink and downlink communication. This is important as it provides more space on CubeSat for solar cells and reduces the interference between the antennas and the electronics inside the CubeSat. Fig. 29 shows the proposed diplexer which consists of three ports: transmission port (on the left), reception port (on the right) and antenna port (in the middle). Fig. 30 shows the proposed monopole antenna which consists of a strip that holds it to the CubeSat's surface. The authors reported a total gain of 2.06 dBi at the receive frequency of 146 MHz (VHF) and 3.35 dBi at transmit frequency of 438 MHz (UHF). They reported reflection coefficients of −18.5 and −21 dB at 146 MHz and 438 MHz, respectively. The main limitation of the proposed deployable monopole antenna is the risk of mechanical failure in the deployment system which might lead to loss of communication with the ground station and hence mission failure. Another limitation is the reported low gains of 2.06 and 3.35 dBi for uplink (VHF) and downlink (UHF) respectively. This only enables short distance communication and low data rate communication.
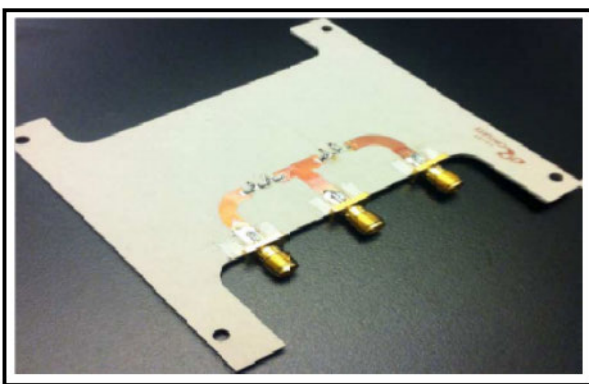

FIGURE 29. Proposed diplexer [39].

Dipole antennas can also be implemented as printed elements placed on the surface of the CubeSat. In [40], Liu *et al.* proposed a cluster of three 3 × 1 printed dipole antenna array for use on 1U CubeSats; see Fig. 31. The main idea is to implement each 3 × 1 subarray on a different CubeSat's surface. This enhances the gain, directivity and
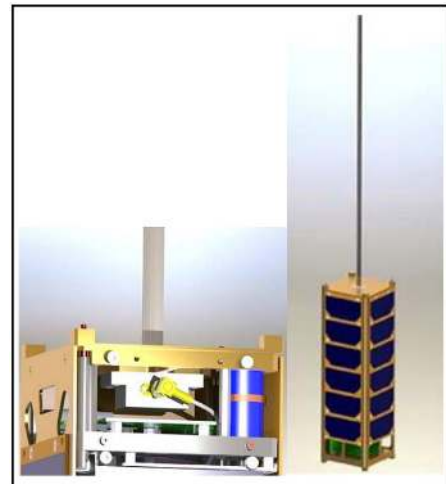
FIGURE 30. Dual band VHF/UHF monopole antenna [39].
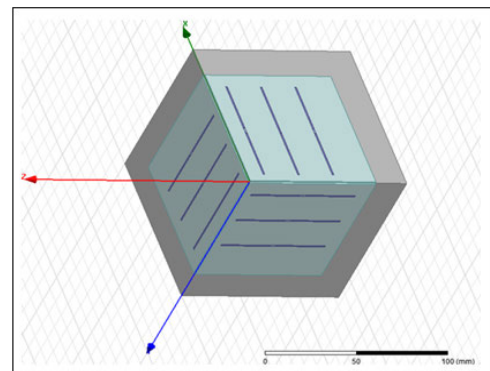
FIGURE 31. Proposed printed dipole antenna array [40].

bandwidth while relaxing the requirements of a deployment mechanism.

The main advantage of the proposed antenna design is its capability of steering the beam electronically which allows for a flexible and reliable communication link. The 3 × 1 dipole antenna array is implemented on 80mm × 80mm ground plane. Each dipole has a length of 62.5mm and a width of 1mm and is parallel with the other dipoles. The antenna achieved a total gain of 5.03 dBi, and a small reflection coefficient of −27.35 dB at 2.45 GHz with a bandwidth, i.e., 4.8%. However, its main limitation is its large size which covers a large area on CubeSat, i.e., 80mm × 80mm on each CubeSat's face. Compared to the designs in [39], [42], the one in [40] does not require a deployment mechanism and has the ability to steer the beam.

In [41], the authors presented a square-shaped printed dipole antenna for 1U CubeSat. As shown in Fig. 32, the proposed antenna consists of four dipoles which are integrated with a phase delay line. To make the antenna operates in a balanced power mode, a balun is added underneath each dipole. The proposed structure leads to a CP which allows a link to be established when re-orienting the CubeSat in space. Moreover, the proposed printed dipole antenna has a total size
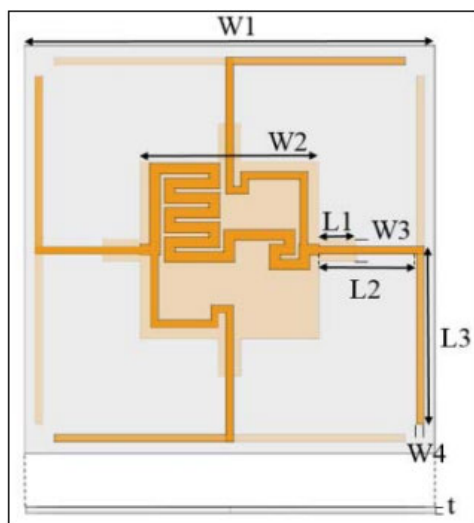
FIGURE 32. Compact square-shaped CP dipole antenna [41].

of 55mm × 55mm and achieved a bidirectional radiation. The antenna has a wide bandwidth, i.e., 33.46% and small reflection coefficient, i.e., −27.5 dB at 2.45 GHz. Moreover, the proposed printed dipole antenna design provides a total gain of 3.49 dBi at 2.45 GHz. The main advantage of the proposed design is its small size and wide bandwidth. In terms of bandwidth, the proposed antenna in [41], has achieved wider bandwidth as compared to the dipole antenna designs presented in [39], [40], [42]. its main limitation, however, is its low gain.

Another dual band antenna design that used the diplexer approach using only one antenna as a transmitter and receiver is proposed. In [42]. Schraml *et al.* proposed a deployable dual band dipole and monopole antennas operating in VHF (144 MHz) and UHF (435 MHz) bands using. A dual-band antenna is used for both uplink and downlink, thus, provides more space on the CubeSat as compared to using two antennas. The authors load the proposed antennas with a LC circuit and used the CubeSat's surface as a ground plane (image method for monopole antenna). Fig. 33 (a) depicts a dual band dipole antenna with a total length of 980mm when it is fully deployed. It achieves a high reflection coefficient of about −14.5 dB at 144 MHz (VHF), −15 dB at 435 MHz (UHF). It also provides a total gain of 2.59 dBi at 144 MHz (VHF) and 3.91dBi at 435 (UHF). As shown in Fig. 33 (b), the authors have also presented a deployable dual band monopole antenna which has a total length of 313.5mm. This monopole antenna design achieves a small reflection coefficient of about −35 dB at 144 MHz (VHF) and −42 dB at 435 MHz (UHF). It also achieved a total gain of 2.14 dBi at 144 MHz (VHF) and 4.35 dBi at 435 (UHF). Compared to a dipole antenna, the monopole achieved a smaller reflection coefficient, higher gain with a reduced length. Compared to the monopole antenna design presented in [39], the antenna design reported in [42] has a smaller size and higher gain for uplink and downlink communications.
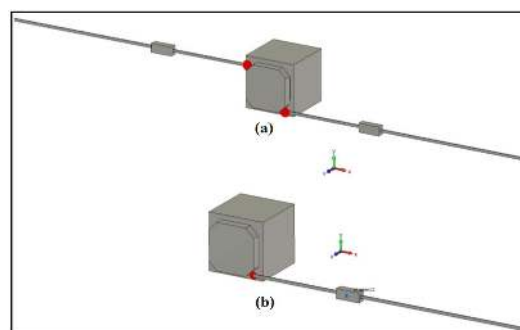

FIGURE 33. Proposed LC-Loaded antenna designs for 1U CubeSat: (a) dipole and (b) monopole [42].

IV. REFLECTOR BASED ANTENNAS

Reflector antennas have a large profile and can provide gains higher than 30 dBi at operating frequency ranging from 0.3 to 300 GHz [44]. Recently, reflector antennas have received considerable attention for higher orbits and deep space CubeSat applications at orbits above LEO and in deep space due to their superior gains which can provide long distance communications. The main challenge is the large size of the reflector antennas making them hard to be integrated on the limited CubeSat volume. To address this challenge, all the reflector-based antenna designs require a deployment mechanism. As shown in Table 6, six reflector-based antenna designs have been proposed for CubeSat, i.e., those in [45]–[50]. These reflector antenna designs achieve very high gains ranging from 28 to 48.7 dBi operating from X-band to W-band. However, their main limitation is their large sizes, which occupies large area on the CubeSat. Another limitation is the complexity of their deployment mechanism. Moreover, compared to the designs in [46]–[48], [50], the design of [49] achieved the highest gain of 48.7 dBi at Ka-band (34.2-34.7 GHz).

The main limitation of existing antenna designs such as dipole and patch antennas that are used for LEO CubeSats is their low gains which makes them unsuitable for deep space communications. In addition, moving from LEO to deep space communications requires a Ka-band or X-band antenna designs that can provide high gains of 42 and 30 dBi respectively. To address the aforementioned challenges, the authors of [45] proposed a high gain deployable reflector antenna for 6U CubeSat deep space communication. The antenna is the first reflector antenna that was proposed for deep space missions operating at Ka-band. The authors used an unfurlable meshed reflector with 32 ribs. The proposed reflector antenna consists of a feed horn, four struts, hyperbolical reflector, and 0.5m deployable mesh reflector. It occupies a size of 100mm × 100mm × 150mm when it is folded. As soon as the CubeSat reaches the specified orbit, the 0.5m mesh reflector deploys. Fig. 34 shows the proposed antenna design after fully deployed with the meshed reflector antennas along with the feed horn in the middle. Moreover, the proposed antenna design achieved an efficient of 60% and a superior gain

TABLE 6. Proposed reflector and reflectarray antenna designs for CubeSats.

Ref	Size ($\lambda_0 \times \lambda_0$)	Operating Frequency (GHz)	Bandwidth $|S_{11}| < -10$ dB (%)	Gain (dBi)	S_{11} (dB) at Center Frequency	CubeSat Type	Deployable	Polarization	Application
[45]	56.70	34 (Ka-band)	n/a	42.8	n/a	6U	yes	-	Deep Space missions
[46]	29.38×7.15	26 (K/Ka-band)	< 0.38	33	n/a	3U	yes	CP	Deep Space missions
	9.34×5.58	8.425 (X-band)	< 1.19	28		6U		RHCP	High Gain Ground Communication
[47]	9.4×16.8	8.425 (X-band)	n/a	29.2	n/a	6U	yes	RHCP	Deep Space missions
[48]	28.73×28.73	86 (W-band)	9.88	34.36	-24	6U	no	CP	High Gain Ground Communication
[49]	28 (diameter)	7.145-7.19 uplink 8.4-8.45 downlink (X-band)	n/a	36.1 dBic uplink 36.8 dBic downlink	n/a	12U	yes	RHCP	Deep Space missions
	106.66 (diameter)	34.2-34.7 uplink 31.8-32.3 downlink (Ka-band)		48.7 dBic uplink 48.4 dBic downlink					
[50]	42.8×42.8	8.4 (X-band)	n/a	39.6	n/a	6U	yes	n/a	Deep Space missions / High Gain Ground Communication
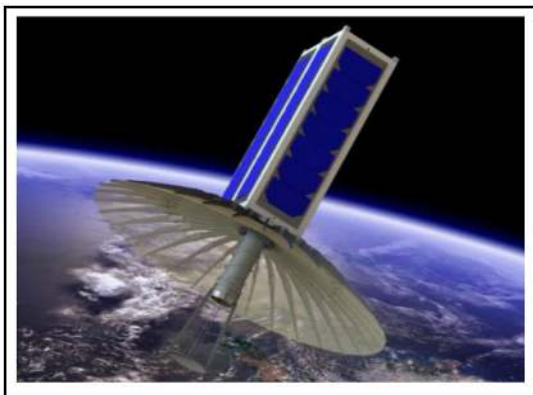
FIGURE 34. Deployable reflector antenna on 6 CubeSat [45].

of 42.8 dBi at an operating frequency of 34 GHz (Ka-band). This is important as it provides long distance communications and significantly enhances the antenna performance. Its main limitation, however, is its complex deployment mechanism which increases the probability of deployment failure and hence failure of the whole mission.

The authors of [46], proposed and described two novel high gain deployable reflect-array antennas for CubeSat. The first design is the Integrated Solar Array and Reflect-array Antenna (ISARA) which operates at 26 GHz (K/Ka-band); see Fig. 35 (a). It consists of three 33.9cm × 8.26cm reflect-array panels and is proposed to be used for 3U Cube-Sat. The second design is a Telecom reflect array antenna that operates at 8.425 GHz (X-band); see Fig. 35 (b). It has a three 33.3cm × 19.9cm reflect arrays and is proposed to provide a bent pipe telecommunication link between the ground station and the 6U CubeSat. The proposed ISARA and MarCO antenna designs provide high gains with extremely low stowed volume in LEO and deep space. They deploy when they reach the orbit. The ISARA proposed antenna design achieves a maximum measured gain of about 33 dBi at 26 GHz; see Fig. 36 (a) and a bandwidth exceeds 0.38 %, while the X-band (MarCO) antenna design achieves a total gain of about 28 dBi at 8.425 GHz; see Fig. 36 (b) with a bandwidth that exceeds 1.19%. In terms of gain, the deployable reflector antenna design reported in [45], has higher gain as compared to the deployable reflect-array designs in [46].

FIGURE 35. Proposed antenna designs: (a) ISARA and (b) X-band reflect array [46].

FIGURE 36. Radiation patterns: (a) ISARA at 26 GHz and (b) MarCO at 8.425 GHz [46].

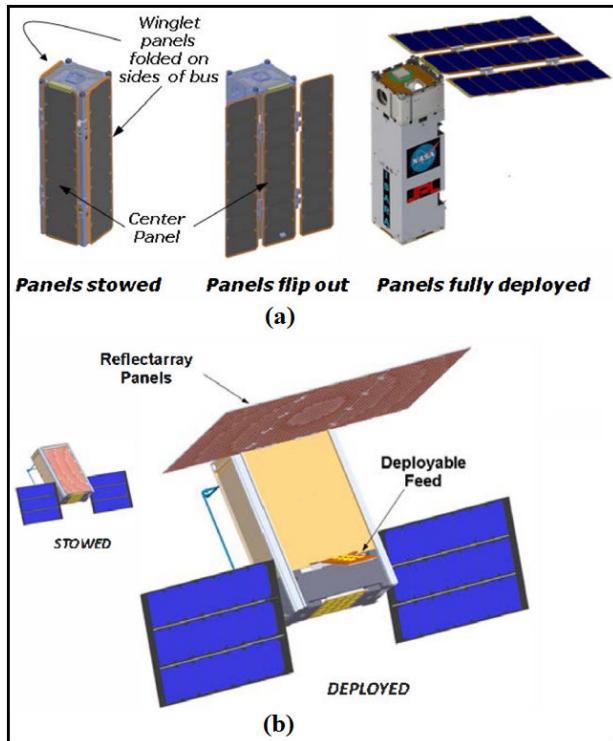In [47], Hodges *et al*, presented the development of X-band deployable folded-panel reflect-array antenna for use on 6U (10cm × 20cm × 34cm) CubeSat that they presented in [46]; see Fig. 37. It has low mass and low cost Folded-Panel Reflect-array (FPR) design that is mounted on the 6U CubeSat. The FPR is stowed by folding the three flat panels against the side of the spacecraft occupying a small stowage volume. As shown in Fig. 37 (a), the proposed antenna occupies a small stowage volume when it is folded consuming about 4% of the applicable spacecraft payload volume. The deployable reflect-array antenna panel consists of three 19.9cm × 33.5cm flat panels folded on one side of 6U spacecraft. These panels are attached to each other using spring-loaded hinges to form a signal panel stack. Fig. 38 (a) and (b) present the reflection coefficient and radiation pattern of the proposed antenna respectively. The authors reported a total gain of 29.2 dBi at 8.425 GHz, reflection coefficient of −32 at 8.3 GHz and an efficiency of ∼42%.

The stowage volume and deployment complexity of reflector antennas are the main challenges for designing such antennas. To address this challenge, Mishra *et al*, proposed a high gain circular polarized feed horn antenna for W-band CubeSat applications [48]. The main idea is to feed an offset parabolic reflector antenna using the horn antenna with electrical dimensions of $7.2\lambda \times 3.9\lambda \times 1.4\lambda$; see Fig. 39 (c). This horn antenna presents a polarizer structure which consists of circular cavities. This is important as it provides LHCP and reduces the overall length as compared to conventional polarizers. Fig. 39. (d), shows the fabricated reflector antenna with
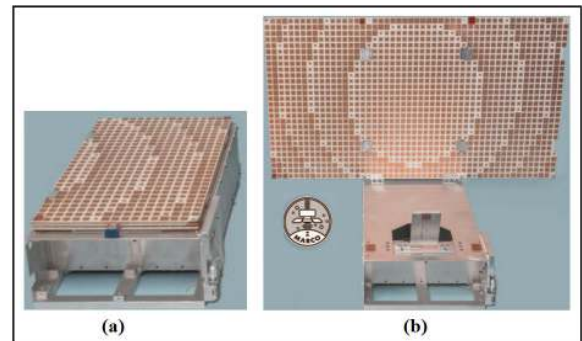
FIGURE 37. The MarCO antenna design: (a) stowed and (b) deployed [47].

the horn feed. This reflector antenna has a diameter of 100mm and can be placed inside 1U CubeSat. Both reflector and horn antennas occupy a volume of 1U CubeSat. Fig. 40, shows the proposed feed horn and parabolic reflector antennas integrated together inside 6U CubeSat's model. The feed horn and reflector antenna achieved a measured reflection coefficient of −24 dB at 83 GHz with a bandwidth of 9.88%. Moreover, the feed horn provided a LHCP gain of about 8.8 dBic at 83 GHz and 9.2 dBi at 86 GHz while the proposed offset parabolic antenna achieved superior measured RHCP gain of about 33.77 dBi at 83 GHz and 34.36 dBic at 86 GHz.
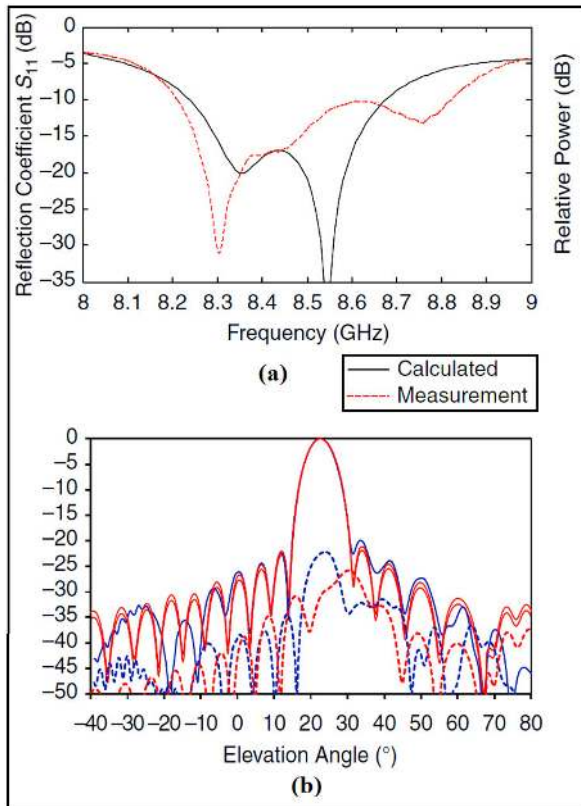
FIGURE 38. Results: (a) reflection coefficient, (b) radiation patterns at 8.425 GHz [47].
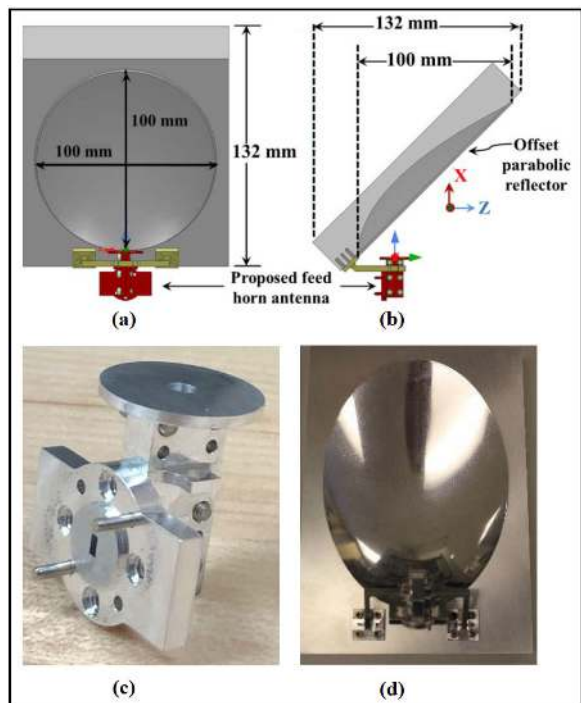
FIGURE 39. Proposed reflector antenna, (a) front view, (b) side view, (c) fabricated feed horn and (d) fabricated feed-reflector antenna configuration [48].

Compared to the designs in [45]–[47], the proposed antenna design in [48] has a smaller antenna size and does not require
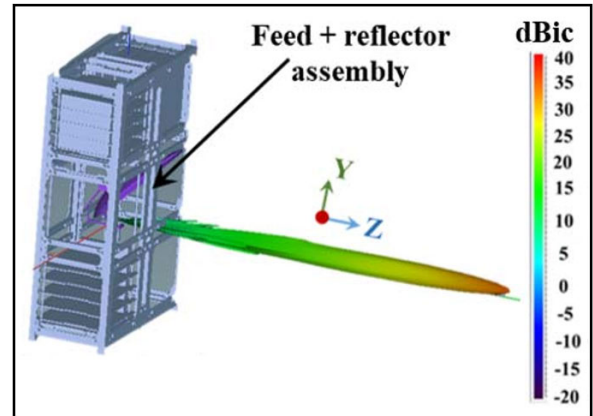
FIGURE 40. Proposed offset parabolic reflector integrated with the proposed feed horn antenna inside the 6U CubeSat Simulation model [48].

a deployment mechanism. However, its main limitation is the weight of the horn antenna.

In [49], Chahat et al, proposed a novel high gain one-meter deployable mesh reflector for deep space network telecommunication; see Fig 41. The proposed antenna is suitable for 12U CubeSat and operates at X-band (i.e., uplink: 7.145-7.19 GHz; downlink: 8.4-8.45 GHz) and Ka-band (i.e., uplink: 34.2-34.7 GHz; downlink: 31.8-32.3 GHz). The proposed antenna allows discovering and exploring of interplanetary space. The challenging part is the design of the deployment mechanism that deploys the mesh reflector when it reaches deep space. Moreover, the antenna is stowed during launch and prior to deployment, occupying a volume of 3U CubeSat. In order to achieve better performance, the authors used a 40 opening per inch (OPI) mesh reflector for Ka-band and a 30 OPI for the mesh grid. As shown in Fig. 42 and 43, the feed is located on 12U Cube-Sat's bus and the boom deploys the 1m mesh reflector away from the feed. The mesh reflector has an effective diameter of 1m and focal length of 0.75m. The proposed deployable mesh reflector antenna provides a high gain at X-band of 36.1 and 36.8 dBic for uplink and downlink frequency bands, respectively. Moreover, at Ka-band, the antenna provides a superior gain of 48.4 and 48.7 dBic for uplink and down-link frequency bands, respectively. Compared to the designs of [45]–[48], [50], the proposed deployable mesh reflector antenna in [49], provides higher gain at Ka-band.

A large area deployable reflectarray operating at X-band was proposed in [50]. The proposed antenna can be stowed in a 4U CubeSat volume and presents a large aperture of 1.5m x1.5m when deployed. The main aperture consists of 4340 crossed dipoles etched on polymide sheet arranged in a rectangular lattice. The lengths of the dipoles are optimized to provide the required reflection phase profile across the aperture and collimate the beam at the desired direction. Furthermore, the aperture is placed 5 mm above the ground plane ensuring a large phase swing and increased bandwidth. The main novelty of this design is the collapsible substrate
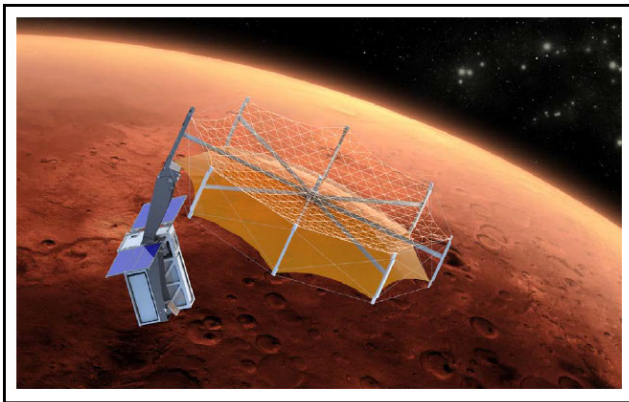
FIGURE 41. Drawing model of deployable mesh reflector [49].

FIGURE 42. Deployment of proposed 1 m mesh reflector [49].
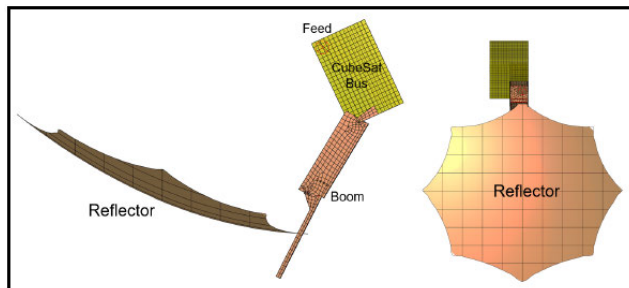
FIGURE 43. Model of proposed mesh reflector antenna on 12U CubeSat [49].

made of quartz-epoxy composite material, which provides the gap between the ground plane and the aperture and allows the reflectarray to be folded and unfolded, see Fig. 44. In addition, the dielectric losses are minimized since there is no dielectric material used in the substrate. Several cycles of RF and packaging tests were performed on the deployable reflectarray, proving that the proposed antenna can achieve a high gain of 39.6 dB at 8.4 GHz while maintaining its planarity and stiffness.

V. HELICAL ANTENNAS

Helical antennas are made of conducting wires with the same or different lengths which are wound in a form of a

FIGURE 44. Large area deployale reflect array [50].

helix and are normally mounted on a ground plane [51]. They are widely used in many satellite applications because they are inexpensive, easy to construct and can provide a circularly polarized radiation. To increase their bandwidths, gains and improve their deployment structures, many techniques and approaches have been presented in [52]–[57]. Amongst all designs listed in Table 7, the design in [54] has the highest gain. However, the use of three helical antennas on one surface of the CubeSat occupies a large area and hence reduces the available area for solar cells. In terms of bandwidth, the design in [52], has the largest bandwidth as compared to all helical antenna designs listed in Table 7. Moreover, the UHF-band design in [53] has higher gain than UHF antenna designs of [52], [56]. However, its size, i.e., 1371.6 x 355.6 mm^2 rules it out for use on 1U CubeSat.

The main limitations of existing dipole and monopole antennas are their low gains and narrow bandwidths. On the other hand, helical antennas can provide high gains by reducing the back-lobe radiation, which might cause an interference with the CubeSat electronics as well [58]–[60]. To reduce the back-loop level, the authors of [52] present a deployable modified helical shaped antenna design for 3U CubeSat. The antenna achieves a unidirectional pattern with a wide bandwidth at UHF. As shown in Fig. 45, the

FIGURE 45. Modified helical shaped deployable antenna for 3U CubeSat [52].

TABLE 7. Proposed helical antenna designs for CubeSats.

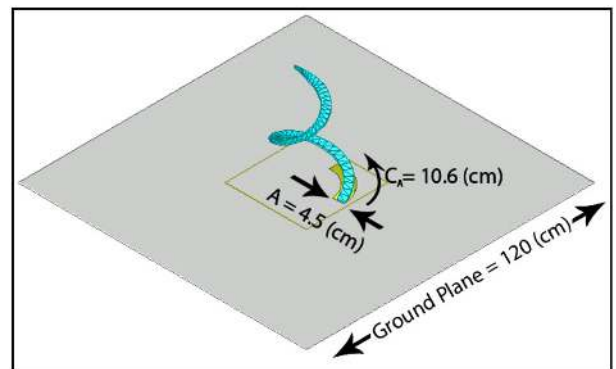| Ref	Size ($_0 \times _0$)	Operating Frequency (GHz)	Bandwidth |S$_{11}$| < -10 dB (%)	Gain (dBi)	S$_{11}$ (dB) at Center Frequency	CubeSat Type	Deployable	Polarization	Application
[52]	0.22×0.22	0.550 (UHF)	78.18	8.44	-20	3U	yes	CP	Ground Communication
[53]	1.83x0.47	0.400 (UHF)	n/a	13	n/a	1.5U	yes	CP	Ground Communication
[54]	3.2×0.8	8	62.5	12 dBic at 6 GHz	n/a	6U	yes	LHCP	Remote Sensing Radiometer
		12	50	20 dBic at 40 GHz					
		34.8	54.58						
[55]	0.35×0.35	0.270	6.15	3.56	-19	3U	yes	CP	Ground Communication
		0.350	6	4.7					
		0.450	4.67	5.41					
[56]	0.12×0.12	0.365 (UHF)	7.12	8.38	-27	6U	yes	CP	Ground Communication
[57]	0.73×0.73	12.2 (Ku band)	16	8.5	-22	1U	no	CP	TT&C/Ground Communication

ground plane of the proposed antenna has large dimensions of 120mm × 120mm after deployment in space. This enhances the bandwidth and increases the total gain by redirecting the back-lobe radiation pattern forward. The proposed CP antenna achieves a wide bandwidth, i.e., 78.18%, high gain of 8.44 dBi and a small reflection coefficient of −20 dB at 550 MHz.

In [53]. Ochoa *et al.* developed a low-profile high gain deployable helical antenna for use on 1.5U CubeSat. The developed antenna operates in UHF band and can be stowed to occupy a total volume of 50mm × 100mm × 100mm (0.5U CubeSat); see Fig. 46 (a). This is achieved by folding and taping the flexible structure of the helical antenna together. Fig. 46 (b) shows the proposed helical antenna after full deployment with a total large size of 1371.6mm × 355.6mm. Compared to the helical antenna design presented in [52], the one reported in [53] has higher gain of 13dBi at 400 MHz (UHF). However, its main limitation is the large size of the proposed antenna which adds an extra weight to CubeSat.

The authors of [54] presented an antenna system which consists of three high gain quasi-tapered helical antennas for 6U CubeSat to monitor Radio Frequency (RF) emission from earth. These antenna designs are conical helix; see Fig. 47 (a), uniform helix; see Fig. 47 (b) and quasi taper helix; see Fig. 47 (c) which operate at frequency bands of 6-11 GHz, 11-22 GHz and 21-40 GHz respectively. The proposed antenna system is mounted on one side of a 6U CubeSat and occupies a surface area of 80mm × 20mm when they are folded. Each helical antenna design has a height of 250mm and a ground plane size of 50mm × 50mm. The proposed antenna system provides high gains ranging from 12 dBi at 6 GHz to 20 dBi at 40 GHz. However, their main limitation is that they occupy large space on the CubeSat.
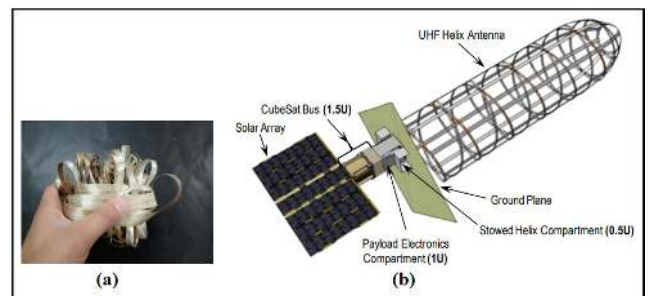
FIGURE 46. Helical antenna: (a) folded and (b) fully deployed [53].

Moreover, the use of three antennas increases the power consumption, complexity, and interference between antennas. In terms of total gain, the helical antenna design in [54] has higher gain than those design presented in [52], [53] but at higher frequency range, i.e., 6 – 40 GHz.

Quadrifilar helix antennas have gained attention recently as a suitable design for satellite communication [61], [62]. This is because they are cheap, simple, and have a good radiation performance. One of the uses of the quadrifilar helical antenna designs is on Global Position Systems (GPS) applications [63], [64]. They provide circular polarization and high gains at a single operating frequency. In [55], Costantine *et al.* proposed a deployable quadrifilar helix antenna for CubeSat. To achieve a circular polarization and increase the bandwidth, they used four twisted arms with the same diameter of 7.12 mm and different lengths, i.e., arm 1 (440mm), arm 2 (392.5mm), arm 3 (350mm) and arm 4 (390mm), to form a helical shape; see Fig. 48. These four orthogonal helices are rotated 90° with respect to each other and are deployed over a 300mm × 300mm rectangular ground plane. The proposed multi-band antenna
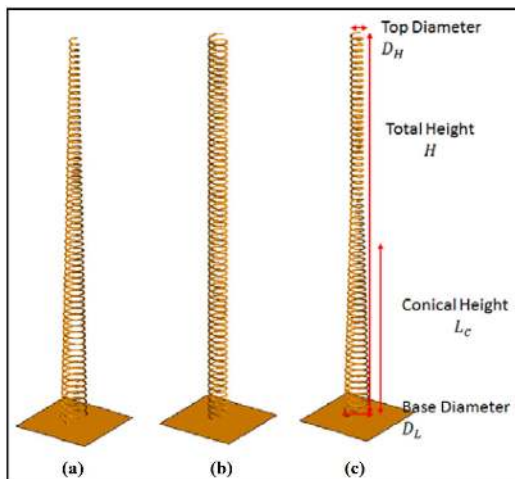
FIGURE 47. A High gain antenna for CubeSat (a) Conical Helix (b) Uniform Helix (c) Quasi Taper [54].
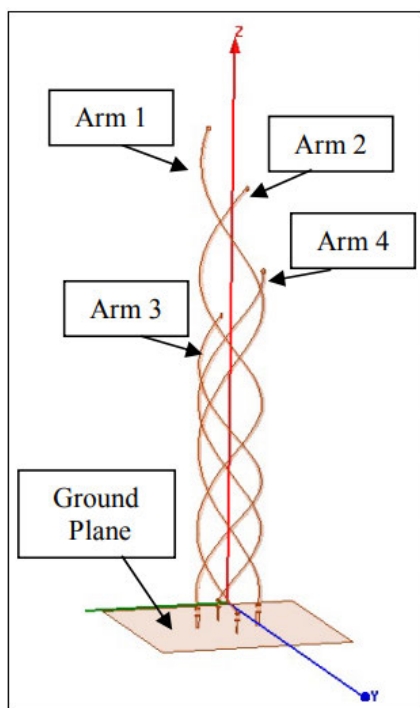
FIGURE 48. Proposed deployable Quadrifilar antenna for CubeSat [55].

operates in the UHF band with frequencies ranging from 270 to 450 MHz. It achieved gains of 3.56 dBi at 270 MHz, 4.7 dBi at 350 MHz, 5.64 dBi at 400 MHz and 5.41 dBi at 450 MHz. The smallest achieved reflection coefficient was −19 dB with bandwidth of 6.15% at an operating frequency of 270 MHz. The maximum −10 dB bandwidth was 6% at 350 MHz and 4.67% 450 MHz. The main limitations of the proposed antenna are its narrow bandwidth (i.e., 6.15%) and large ground plane which makes the proposed antenna unsuitable for 1U and 2U CubeSat. Compared to the designs in [53], [54], the one reported in [55] has much smaller size.

Another UHF deployable quadrifilar helical antenna design for a 6U CubeSat is presented in [56]. As shown in Fig. 49, the proposed antenna consists of four conductive beryllium arms with the same length and rotated 90° with respect to each other. This is important as it leads to a circular polarization which is an important feature as it helps establishing communication links between satellites and ground station regardless of the antenna orientation. Moreover, the authors proposed an effective structure that leads to an efficient packaging and deployment mechanism. This reduces the probability of deployment failure. The proposed antenna has a height of 500mm with a diameter of 115.2mm and when it is folded it can fit inside a 2U CubeSat (100mm × 100mm × 200mm). The authors reported a bandwidth of 7.12% ranging from 352 to 378 MHz, with a reflection coefficient of about −27 dB and a total gain of 8.38 dBi at operating frequency of 365 MHz (UHF). The proposed antenna achieved high gain, small reflection coefficient, small size and wide bandwidth as compared to the quadrifilar helix presented in [55]. However, its main limitation is the resulting narrow bandwidth of 7.12%.
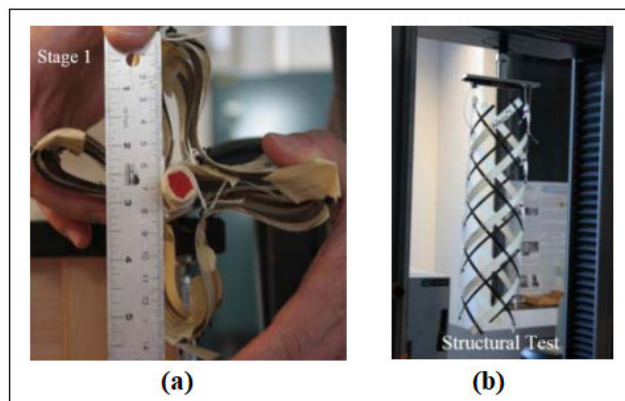
FIGURE 49. Proposed deployable helix antenna. (a) fully folded and (b) fully deployed [56].

The main limitations of existing Monofilar Square Spiral Antennas (MSSA) antennas is their large size and hence they cannot be used for CubeSat [57]. To address the aforementioned limitations, the authors in [57] proposed a low profile and wide bandwidth printed Monofilar Square Spiral Antenna for micro and CubeSat satellites; see Fig. 50. The key idea is to use a simple and low-cost square cavity which leads to a significant increase of the antenna total gain by redirecting the back-lobe radiation forward. It also leads to a significant reduction of the total size, i.e., 15mm × 15mm with a square cavity's size of 18mm × 18mm × 14mm, which in turns provides more space for solar cells. To address the issue of high impedance matching, e.g., >50 Ω, the authors offset the feeding position of the probe and added a short stub for matching. This leads to a 50 Ω input impedance matching and an enhancement in the impedance bandwidth. The results show that the proposed MSSA antenna with cavity achieves a high gain of 8.5 dB at 12.2 GHz (Ku-band).

TABLE 8. Proposed other antenna designs for CubeSats.

Ref	Size ($\lambda_0 \times \lambda_0$)	Operating Frequency (GHz)	Bandwidth $|S_{11}| < -10$ dB (%)	Gain (dBi)	S_{11} (dB) at Center Frequency	CubeSat Type	Deployable	Polarization	Application
[65]	0.72×0.72	2.4 (S-band)	n/a	25	n/a	3U	yes	n/a	High-speed data downlink Deep Space Missions
[66]	2×4	7.5	11.11	16.6	-37 at 6 GHz	6U	yes	n/a	High-speed Data Downlink
[67]	n/a	47.1,80,140, 249,309	n/a	20	n/a	3U	no	LP	Remote Sensing mm-wave Polarimeter
[68]	n/a	91,165,176, 180,183	n/a	16-18	n/a	6U	no	n/a	Remote Sensing mm-wave Radiometer
[69]	58.9	883	n/a	n/a	n/a	3U	no	LP	Remote Sensing Sub-mm-wave Radiometer
[70]	n/a	0.435 (UHF)	12.18	11.5	-19	1.5U	yes	LP	Ground Communication
[71]	n/a	2.47 (S-band)	5.42	6.41	- 26.47	3U	no	LP	Ground Communication
[72]	2.52×1.24	0.437 (UHF)	5	4.1	-22	n/a	yes	n/a	Ground Communication
[73]	5 (radius)	32	6.35	24.4	-17	n/a	no	RHCP	Deep Space Missions
[74]	56×56	94 (W-band)	93-95GHz	31.9 directivity	< -15	1U	no	n/a	Remote Sensing
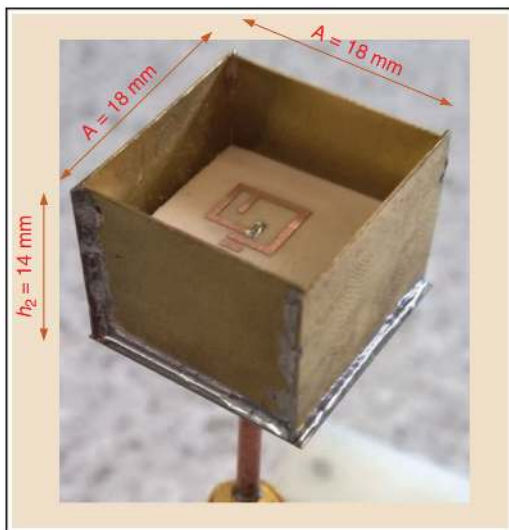
FIGURE 50. A wideband printed monofilar square sprial antenna for microsatellites and CubeSats [57].

MSSA also provides measured reflection coefficients of -27 dB at 13 GHz and -24 dB at 14 GHz with -10-dB bandwidth of 15.57%.

VI. OTHER ANTENNAS
Different techniques and approaches have been applied to different antenna types to enhance their performance for use on CubeSat. As shown in Table 8, these antenna designs include inflatable reflector [65], horn antenna [66], millimeter and sub-millimeter wave antennas [67]–[69], Yagi-Uda antennas [70], [71], meanderline antenna [72], and metasurface antennas [73], [74].

A. INFLATABLE REFLECTOR ANTENNAS
Existing dipole and monopole antennas that are proposed for CubeSat communication in LEO have a maximum gain of about 6 dBi and operate in frequencies ranging from VHF to S-band. These antennas are cheap and easy to build; however, they are not suitable for deep space applications which require high gain, i.e, >24 dBi and high date rate to provide a communication link with the ground stations. To address this limitation, the authors of [65] propose the use of an inflatable reflector with a patch antenna. The authors claim that they presented the first developed high gain inflatable antenna design for deep space CubeSat communication. This is important as using CubeSats to explore deep space and carry out scientific experiments might be cost effective. As shown in Fig. 51 (a) and (b), the proposed antenna is made of an inflatable reflector (conical or cylindrical shape) of 1m in diameter which proposed to be attached at the back of a 3U CubeSat. This reflector occupies a small space on the Cube-Sat when it is folded and provides a large reflector dish when it is deployed at space and hence achieves a superior gain of about 25 dBi. A patch antenna of a 90mm × 90mm is used
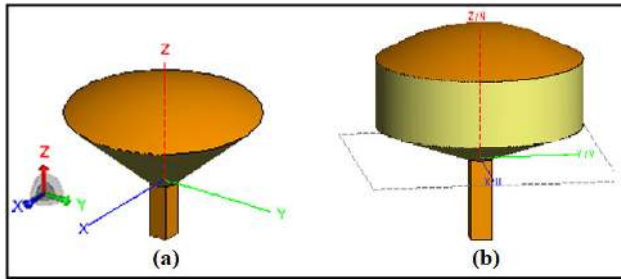
FIGURE 51. Model of the proposed inflatable antenna with dielectric structure modelled in (a) conical shape and (b) cylindrical shape [65].

to feed the parabolic reflective surface. The proposed antenna provides a maximum gain of 25 dBi. This high gain enables CubeSats to establish long distance communications links as required by deep space missions, transmit data at a higher rate and from a further distance. However, its main limitation is the large volume of the reflector after deployment which add weight to the CubeSat.

B. HORN ANTENNAS

Horn antennas with pointing mechanisms have been used by micro and large satellites for communication with ground station because of their unidirectional pattern and superior gains [75], [76]. However, the limited area on CubeSats make it difficult to use such an antenna for CubeSat communication with the ground station.

In [66], Gupta *et al.* proposed a high gain and deployable Vivaldi-fed Conical horn antenna that operates in frequency ranging from 2 to 13 GHz with a wide −15 dB bandwidth of 11.11% for use on a 6U CubeSat (10cm × 20cm × 34cm). The proposed antenna is made up of very light and stiff material that makes the antenna able to fold and deploy autonomously. This is important as it addresses the weight and size limitations on CubeSat. To achieve a wide impedance matching and a circular polarization, the antenna structure includes two Vivaldi shaped fins orthogonal to each other; see Fig. 52. The proposed antenna achieved a high gain ranging from 10 dBi to 17.5 dBi over a frequency band ranging from 2 GHz to 13 GHz. It provides a gain of 12 dBi at 6 GHz, and 17.5 dBi at 9 GHz. The proposed antenna achieved an ultra-wide −10 dB bandwidth of 11.11% ranging from 2 to 13 GHz with a small reflection coefficient of −37 dB at 6 GHz and −23 dB at 10 GHz. The main advantage of the proposed antenna is its ultra-wide bandwidth and high gain, which the possibility of high data rate and long-distance communications. Compared to the inflatable reflector antenna design in [65], the conical horn antenna design presented in [66] has wider bandwidth, smaller reflection coefficient and antenna size but lower total gain.

C. MILLIMETER AND SUB-MILLIMETER WAVE ANTENNAS

Millimeter and sub-Millimeter Wave antennas have been used on CubeSats for remote sensing applications as indicated by [67]–[69]. CalSat is an implementation of a remote
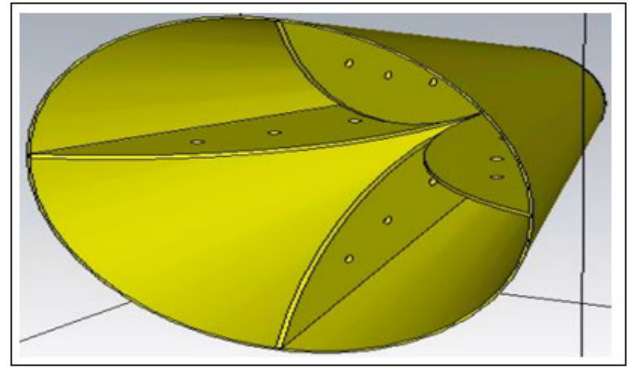
FIGURE 52. The proposed deployable Vivaldi-fed conical horn antenna [66].

sensing CubeSat application employing millimeter-wave horn antennas as its sensing instrument [67]. More specifically, five horn antennas were used to realize a space-based millimeter-wave calibration measurement to be used in cosmic microwave background polarization experiments as seen in Fig. 53. Each conical horn antenna is fed by a rectangular single-moded waveguide as well as a Gunn diode and a passive multiplier, resulting in 47.1, 80, 140, 249 and 309 GHz coherent linearly polarized beams, respectively. The gain of each horn was approximately 20 dBi with low cross polarization levels of −60 dB when a wire-grid polarizer was installed at the aperture.
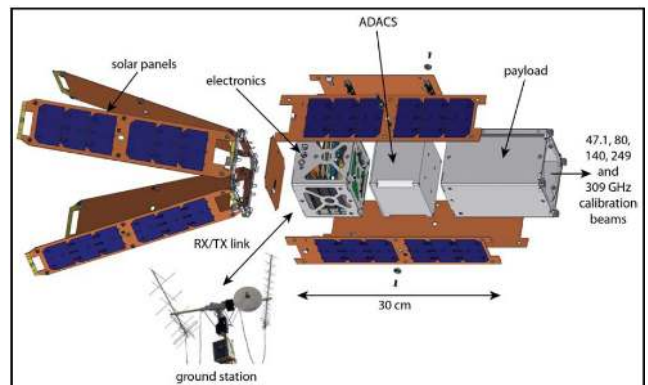
FIGURE 53. CalSat subsystems including antenna subsystem [67].

Another example of a remote sensing CubeSat mission is the Temporal Experiment for Storms and Tropical Systems also known as TEMPEST [68]. TEMPEST comprises of a CubeSat constellation of 5 CubeSats each equipped with a five-frequency mm-wave radiometer operating at 91,165,176,180 and 183 GHz able to provide an 825km wide swath from 400km altitude. The goal of TEMPEST was to study the time evolution of clouds and identify the conditions for transition to precipitation. Therefore, the CubeSats in the constellation are placed 5-10 mins apart to provide a temporal information of 5 successive measurements at five-minutes intervals. As shown in Fig. 54, the radiometer fits in a 3U CubeSat volume and uses a scanning reflector and a
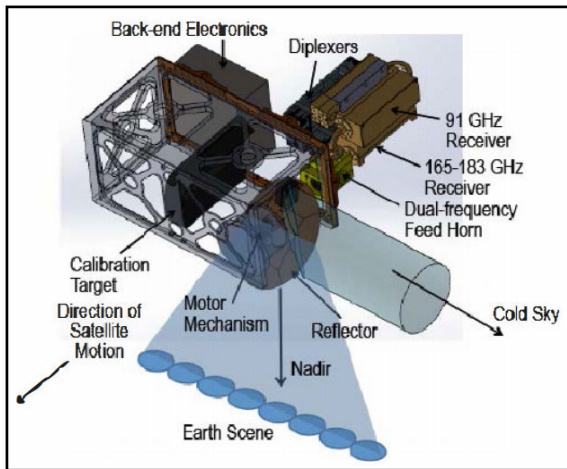
FIGURE 54. The TEMPEST millimeter-wave radiometer instrument on 3U CubeSat scans at 30 rpm [68].

dual frequency feedhorn which is connected to two receivers operating at 91 and 165-183GHz, respectively.

The design of [69] is IceCube which was proposed for remote sensing mission. IceCube is a sub-millimeter wave radiometer operating at 883GHz and its mission was to detect ice content in clouds. It was the first time that this frequency was used in LEO generating the first ever global ice map. As shown in Fig. 55, the payload instrument fits in a 3U CubeSat and it comprises of a 2 cm offset parabolic reflector which is able to cover a 10km 3-dB footprint and a feed horn operating at 862-886GHz.
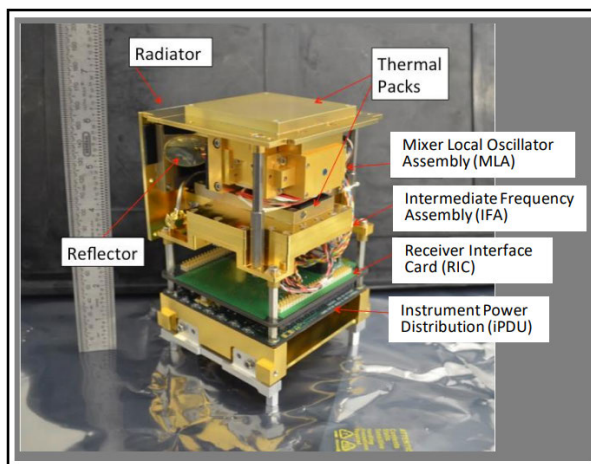
FIGURE 55. IceCube miniature radiometer [69].

D. YAGI-UDA ANTENNAS

The main limitation of many existing antenna designs that are used for CubeSats and operate at low frequency (UHF band) such as dipole antennas is their small gains. To address the aforementioned limitation, the authors of [70], designed a Yagi-Uda antenna that provides a superior gain at 435 MHz (UHF) for CubeSat communication. The main idea is to

include six linear elements of Yagi-Uda antenna with a deployable solar system; see Fig. 56. This system is called extendable Solar Array System (XSAS) and it can be stowed into a volume of 100mm × 10mm × 150mm (1.5U). When the antenna is completely deployed, it will approximately extend to 1.2m providing a high gain of 11.8 dBi at 435 MHz. The proposed XSAS achieved a bandwidth of 12.18% and small reflection coefficient of −19 dB at 435 MHz. However, its main limitation is the large antenna size that results in a non-negligible effect on the limited area on CubeSat for payload and solar panel installation.
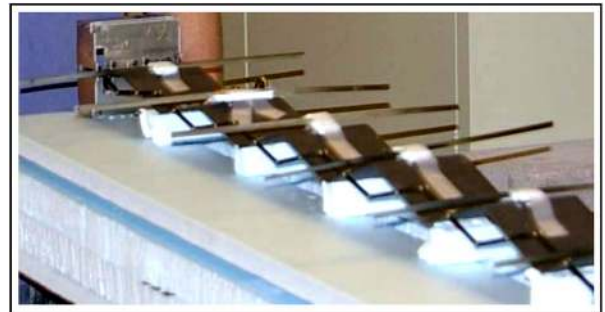
FIGURE 56. Proposed extendable Yagi-Uda antenna for CubeSat [70].

Another Yagi-Uda antenna design is proposed in [71] for use on 3U CubeSat. The proposed antenna is simple and is printed on board to avert deployment mechanism. The authors used the surface of a CubeSat as a reflector to redirect the back-lobe pattern forward to increase the total gain. The back lobe is reduced because of the large 3U CubeSat's surface and hence a unidirectional pattern is achieved. As shown in Fig. 57, the printed Yagi-Uda antenna has a total size of 150mm × 100mm and is mounted on a 3U CubeSat. The proposed antenna achieved a good impedance matching with a small reflection coefficient of - 26.47 dB at the desired frequency of 2.47 GHz, and a −10dB impedance bandwidth of 5.42%. It also provides a total gain of 6.41dB at 2.47 GHz. Its main limitation is that it occupies a large surface area on the CubeSat. Compared to the designs proposed in [65], [66], the printed Yagi-Uda antenna design in [71] has smaller size and its structure is less complex as it does not require a deployment mechanism.

E. MEANDER LINE ANTENNAS

The authors of [72] presented a low profile deployable UHF meanderline antenna for CubeSat. To address the limitation of large size antennas at low operating frequencies, i.e., UHF, the authors used meandering and miniaturization techniques to reduce the antenna's size and increase its bandwidth. This is important as it leads to miniaturization without affecting the antenna's radiation performance. Fig. 58 (a) and (b) show the proposed flexible meanderline antenna design in flat and bent configuration, respectively. The proposed antenna operates at 437 MHz and has a deployment mechanism based on flexible Nylon material. The antenna design achieved a
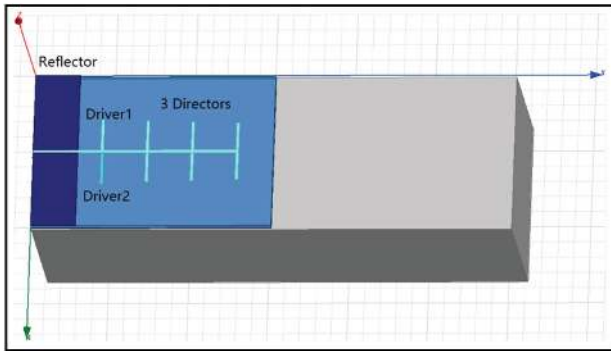
FIGURE 57. Proposed printed Yagi-Uda antenna array for CubeSat [71].
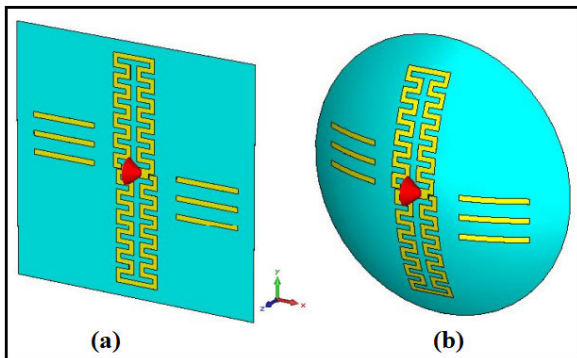
FIGURE 58. Deployable flexible meanderline antenna. (a) flat configuration (b) bent configuration [72].

bandwidth of 5% and reflection coefficient of −22 dB at 437 MHz (UHF) while in a flat configuration, it provides a smaller bandwidth of about 3.66% and a high reflection coefficient of −14.12 dB. Moreover, for the bent configuration, the antenna provides a total gain of 4.1 dBi while in the flat it achieves 3.88 dBi. The main limitation of this proposed antenna designs is its narrow bandwidth.

F. METASURFACE ANTENNAS

Recently, the concept of metasurface (MTS) antennas have been considered for CubeSat applications [73], [74]. MTS antennas have been considered for CubeSat applications [73], [74]. MTS antennas provide low profile and low mass characteristics which can be beneficial for CubeSat applications. A metal-only modulated metasurface is reported by the authors of [73]. The main benefit of the MTS antenna from a CubeSat point of view is that the radiation aperture as well as the feed are co-located in the same plane. The radiating aperture consists of elliptical cylinders with different orientations, heights and ratios arranged in a square subwavelength lattice; see Fig. 59 (a) and (c). The feed is a circular waveguide that launces a TM surface wave which interacts with the periodically modulated surface reactance, thus giving rise to leaky wave radiation. The MTS antenna is able to control both the aperture field as well as the polarization due to the space-dependent anisotropic reactance obtained by the elliptical geometry of the unit cells. A prototype of the
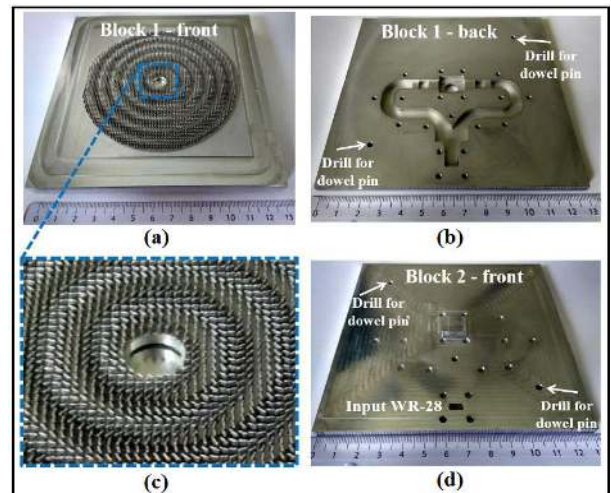
FIGURE 59. Fabricated MTS antenna, (a) front view of Block 1 with MTS element and the circular waveguide feeder, (b) back view of block 1 with the waveguide divider and the matching sections, (c) zoom to central region of (a), and (d) front view of block 2 with RW input [73].

MTS antenna was manufactured from aluminium using metal additive manufacturing process and CNC milling. The MTS was able to generate a RHCP pencil beam in the frequency range of 30.8-32.3GHz (Ka-band) with a maximum gain of 24.4 dB at 31.5GHz. The metallic structure of the MTS antenna ensures no dielectric losses or electrostatic discharge issues. Its high gain performance and low profile highlights its feasibility for space and deep-space CubeSat applications.

Along similar lines, a Si/GaAs holographic metasurface antenna for CubeSat applications was proposed in [74]. The antenna, as shown in Fig. 60, operates at 94 GHz and can generate 3 different beams in azimuth with 45° spacing using the same aperture. The operating principle of the antenna is
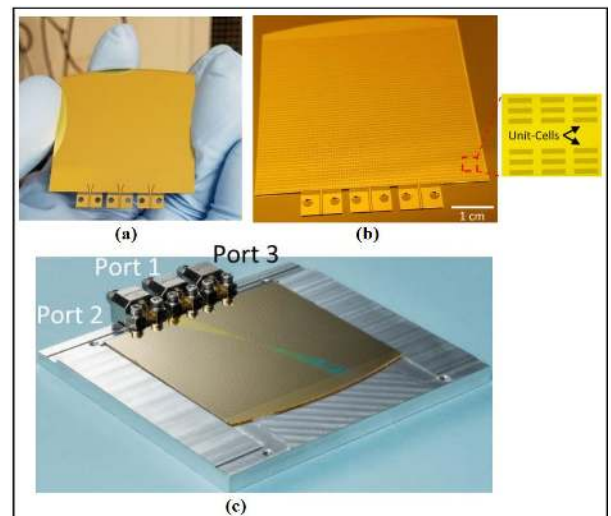
FIGURE 60. Proposed Si/GaAs Holographic metasurface antenna, (a) silicon wafer in the middle of through-etch, (b) the etched metasurface layer onto substrate and (c) fabricated Si/GaAs metasurface antenna placed on a supporting structure [74].

based on the holographic approach where the reference-wave is represented by a guided mode generated by a quasi-optical pillbox beamformer. This reference wave excites the meta-surface layer consisting of subwavelength slot-shaped unit cells to achieve an objective function which is the aperture field of interest. The pillbox structure consists of 4 layers with two substrate layers of Si and GaAs and 2 conductive layers. On top of the pillbox, a metasurface layer is placed giving a total antenna thickness of 525 microns. Furthermore, a parabolic reflector is embedded in the pillbox, coupling the Si and GaAs layers. The proposed antenna is fed by a three CPW ports where each port excites a SIW H-plane horn via a CPW to SIW waveguide transition located in the Si layer. The pillbox coupler is responsible for transforming the cylindrical waves by the SIW horns to plane waves having the desired phase gradient. Following that, a guided mode on the GaAs layer (located on top of the Si layer) will couple to the slots of the metasurface layer, hence radiating into free space. The antenna was fabricated in JPL utilizing a variant of a semiconductor micromachining process. The main challenge faced during fabrication was the vertical parabolic reflector rim used as coupling between the two substrate layers. The antenna operates from 93 GHz to 95 GHz with good isolation between the ports and frequency dependent radiation direction. Three different beams were generated by switching between the three feeding ports with a maximum directivity of 31.9 dBi reported at 94 GHz. Finally, the proposed metasurface antenna can be used as an electrically large high gain flat metasurface antenna architecture which can be scaled to other frequencies for a variety of applications.

VII. CHALLENGES AND APPROACHES

From the current literature on CubeSat antennas, several challenges such as high gain, operational bandwidth, small size, low mass and circular polarization have been identified as outlined in Table 9. In this section, each of these challenges will be presented and analyzed according to different approaches that address these challenges. The suitability of each approach for each antenna type as well as the performance improvement/achievement gained by the approach are summarized in Table 10.

A. HIGH GAIN

1) CAVITY

High gain antennas provide long distance communications, and they can be used for intersatellite links. A popular approach that improves the antennas' gains is the cavity technique. More specifically, a cavity backed technique is used to suppress and eliminate the surface waves, hence a smoother radiation pattern is achieved. It also suppresses the back-lobe radiation improving the antenna's directivity and gain. Another technique is the use of a MSS as a resonant cavity model where the resonant cavity is formed by the metasurface and ground plane. As a result, the total gain is improved, and the back-lobe pattern is reduced. The main

TABLE 9. Antenna design challenges for CubeSats.

Current challenges	Performance
High gain	Intersatellite communications Deep space missions High speed data downlink
Wide bandwidth and Multiband	Increased throughput Single antenna operating at different frequencies (i.e., up/downlink) Remote Sensing applications
Small size and low mass	Low cost, fast prototyping Sufficient real estate for solar panel Reduce weight budget
Circular polarization	Eliminating polarization mismatch losses due to antenna misalignment Reduce the effect of Faraday rotation High link reliability Intersatellite communications

limitation of the cavity approach, however, is the increased total antenna profile and weight as a consequence of the used cavity. The authors of [23], [25], [35]–[38], [57] used different types of cavity approaches that include fabry-perot cavity, metallic walls, cavity slot (meander lines), resonant cavity and cavity reflector. They reported gains ranging from 4-15 dBi and bandwidths ranging from 2.05-40% at different operating frequencies, i.e., UHF-band, S-band, X-band and Ku-band.

2) SUBSTRATE INTEGRATED WAVEGUIDE (SIW)

This approach was firstly introduced by the authors of [77] and [78] in 2005 and 2007; respectively. SIW is a waveguide in a rectangular structure and it is constructed using two slots embedded in a substrate which is sandwiched by two parallel metal plates. Compared to conventional waveguides (i.e., CPW, strip lines), the SIW approach has low loss (high Q-factor), and it allows for integration of microwave and millimeter wave passive and active components on the same substrate dielectric. The other advantage of SIW is its ability to control the surface waves at high operating frequencies and hence increases the antenna efficiency. The SIW approach was adopted by antenna designs that are suitable for different applications that include satellite, radar, RF, ISM-band, and Ku-band applications. However, the main limitation of SIW is the dielectric loss which is considered the largest loss component of transmission losses. In [34], the authors proposed SIW slot antenna array for intersatellite communications. The proposed antenna operates in the C-band and provides a gain of 4.98 dBi. However, its bandwidth is narrow, i.e., 1.99%.

3) INFLATABLE, FOLDABLE AND FLEXIBLE STRUCTURES

The antenna gain is proportional to the aperture size, making the integration of high-gain antennas such as reflectarrays, patch arrays and reflectors on CubeSats a challenging task. Therefore, the CubeSat community has adopted several techniques to fit a large aperture inside the CubeSat that can be deployed once in orbit. Such techniques involve, folding of

TABLE 10. Approaches used to address antenna design challenges for CubeSat.

Approach	Antenna Type								Performance Achievement
	Patch	Slot	Monopole Dipole	Yagi Uda	Helical	Reflector	Reflectarray	Horn	
Shorting pins, walls or vias [11, 19]	✓								Bandwidth Miniaturization
Cavity [35-38, 57]		✓			✓				Gain
Aperture coupled and Stacked patch [12, 17, 25, 27]	✓								Bandwidth
Substrate Integrated Waveguide (SIW) [34]		✓							Gain
Quadrifilar structure [55, 56]					✓				Multiband Bandwidth
Inflatable, foldable or flexible [20, 45-47, 53, 55, 65, 72]	✓				✓	✓	✓		Gain Weight Reduction
Solar panel integration and transparent [13, 15, 16, 18, 22, 23, 26, 35, 46, 70]	✓	✓		✓					Solar cell real estate
Meandering [24, 28, 72]	✓								Miniaturization
Mesh grid [45, 49]						✓			Weight Reduction
Polarizer [48, 49]							✓	✓	Circular Polarization
Subwavelength periodicity [46, 47, 50]							✓		Gain Bandwidth
Corner-truncated and Sequential feeding [11, 13, 14, 17, 18, 27, 47]	✓						✓		Circular Polarization
Diplexer and LC loading [39, 42]			✓						Reduced number of antennas Multiband

the aperture or use collapsible substrates as in the case of reflectarrays [47], [50], using copper etched membranes to implement patch antenna arrays [20] or replacing the traditional reflectors with inflatable volumes [65]. Using the aforementioned techniques high gains in the excess of 30 dBi can be achieved, greatly expanding the CubeSat capabilities from LEO to interplanetary exploration. However, there are several factors such as the hinges on the folded panels or the surface roughness and planarity of the flexible materials used that could potentially degrade the RF performance of the antenna.

B. BANDWIDTH

1) SHORTING PINS

One of the well-known effective techniques for enhancing patch antennas' bandwidth and reducing their sizes is the use of shorting pins and walls. Placing these shorting pins at the edge of the patch lowers the first resonant frequency mode and hence widens the bandwidth. They are also used to achieve antenna miniaturization by increasing the patch antenna effective electrical length. However, one of this approach's limitation is that the impedance bandwidth is significantly affected by the spacing between the shorting pins and the feeding probe. One solution to address this drawback can be by placing the pin in the proximity to the feed-point to achieve good matching between the input impedance and the 50 ohms feeding line. To that end, there is a need for wideband antenna designs for different small satellites' applications that require downloading more data at high speed [9]. These applications include remote sensing where images are downloaded from the satellite to the ground station. The authors of [19] applied the shorting pins approach to their F-shaped patch antenna design which is proposed for communication with the ground station. They reported a wide impedance bandwidth of 45.75%.

2) APERTURE COUPLED AND STACKED STRUCTURE

This approach was introduced by D. Pozar in 1985 [79]. It was proposed for microstrip slot antennas to improve their bandwidths. The main idea of this feeding technique is to separate the microstrip feedline from the radiating patch element by placing a ground plane between them. The upper substrate contains the radiating element, and the low substrate contains the feed-line and hence there is no direct connection between the radiating patch element and the feed-line. This approach has been developed and improved by researchers to enhance the performance of the aperture coupled microstrip antennas. The development includes achieving impedance bandwidths ranging from 5-50%, integration and use for active arrays and introducing different shapes (i.e., patch shape, radomes, feed line type, etc). Aperture coupled microstrip antennas are used for integrated phased array systems. It is also proposed and suitable for satellite communications including CubeSats. One of the limitations of using this feeding approach is the use of two different substrate layers which leads to an increase in the antenna total size and complexity. Moreover, the aperture coupled feeding can be combined with the concept of stacked patches where the top patch element is considered as parasitic. Hence, the coupling of resonances between the bottom fed patch and the top patch provides the broadband behavior as in the case of the X-band array on [27] that reported a bandwidth of 15.9%. For CubeSat applications, the authors of [12], [25] used the aperture coupled feeding technique to enhance the bandwidth of their antenna designs. The design of [12] operates at X-band and reported a bandwidth of 16.21% while the design of [25] operates at S-band and reported a wide bandwidth of 32.6%.

3) QUADRIFILAR STRUCTURE

Quadrifilar approach was introduced by Kilgus in [80]–[82] for helical antennas. QHA structure contains orthogonal

quadrifilars which are rotated 90° with respect to each other. This is an important structure as it provides CP and enhance the bandwidth. The helices of QHA are fed by a power divider such as Wilkinson divider. The main limitation of QHA is its large profile. QH antennas are proposed for satellite and ground station applications where their radiated energy is concentrated in a cone shape. The authors of [55] and [56] proposed QH antennas for use on 3U and 6U CubeSats; respectively, to provide communications with ground station. They provide a CP and bandwidth ranging from 6.15 to 7.12%.

4) SUBWAVELENGTH PERIODICITY

Subwavelength periodicity is a well know technique used in reflectarrays to increase the gain bandwidth of the antenna where the reflectarray elements or unit cells are arranged in a grid with a spacing less than half wavelength [83]. In all the reported CubeSat reflectarrays the technique of subwavelength periodicity is used to satisfy the gain bandwidths of each design allowing CubeSat to be used in deep space missions [46], [47], [50]. Nevertheless, when this technique is used, the fabrication tolerances of the reflectarray elements become strict which can result in a reduced reflection phase range and hence gain degradation [84].

C. SMALL SIZE AND LOW MASS

1) SOLAR PANEL INTEGRATION

Solar panels are one of the most important subsystems onboard CubeSats as they provide the required power to the rest of the satellite's subsystems. The amount of solar energy gathered is proportional to the surface area occupied by the solar cells, therefore, it is crucial to reserve enough real estate for solar panel installation. Solar panel integrated or transparent antennas is one of the most popular approachs of antenna designs that cater for mass and size reduction. The main benefit of this approach is that the CubeSat real estate is shared among the antenna and the solar cell subsystems of the satellite without sacrificing extra payload volume. Furthermore, this approach is mainly suitable for patch [13], [15], [16], [18], [22], [23], [26], reflectarrays [46] and Yagi-Uda [70] antennas and it can be realized in two different ways [85]. The first way is by using optically transparent substrates and meshed patches as the radiators and the second way is direct installation of the antenna as slots in between the solar cells gaps or behind the solar panels. The most important factor to consider, is maintaining the optical transparency of the antennas above 90% to ensure that the efficiency of the solar cells is kept on high levels. On the other hand, from an RF point of view, the effect of the solar cells as lossy substrate must be considered in the gain performance of the antenna.

2) MEANDERING

The meandering technique is applied for patch antennas to achieve antenna miniaturization without increasing antenna operating frequency. The meanderline geometry is formed and shaped by folding and bending the conductors back and forth and hence reduce the antenna size. The meander line can be considered as an equivalent inductor and the parameters of its shape control the antenna performance [86]. The antennas that use the meander-line technique provide wide bandwidths and occupy small surface area on the communication system. They are also used for different applications, include RFID in health care applications [87] and satellite communications. Their main limitation, however, is that the inductor equivalent models of the meander-line do not offer flexibility for changing the spacing between meander-line sections. In [24], [28], [72], the authors used the meander-line approach to achieve miniaturization and good antenna performance. They reported bandwidths ranging from 5-28.7%, and antenna sizes ranging from $0.46\lambda_0 \times 0.20\lambda_0$ to $2.52\lambda_0 \times 1.24\lambda_0$.

3) MESHGRID

Meshing reflector apertures is an attractive approach used in CubeSat reflector-based antennas [45], [49]. The idea behind this technique is to approximate the parabolic surface of conventional reflectors by a mesh. This leads to weight reduction and ease the stowage and deployment mechanism of the reflector antenna. Moreover, mesh reflectors allow for electrically larger apertures that have never been attempted on CubeSat as in the case of the 1-m dual band mesh reflector proposed in [49]. Consequently, the achievable gain can exceed 40 dBi at Ka-band. In terms of RF performance, the presence of supporting ribs or structures and the surface mesh (OPI) of the reflector must be considered. Also, when the frequency is increased, e.g., Ka-band, the surface accuracy of the mesh and the thermal distortion become critical metrics that must be included during the antenna simulation and accounted for in the required radiation pattern.

4) DIPLEXER AND LC LOADING

A diplexer makes each antenna works as a transceiver and hence reduce the number of antennas. This will also allow for transmission and reception at different operating bands. A diplexer consists of different filter type (i.e., low pass, high pass and band pass) at different frequencies to sufficiently separate the inputs and outputs. Diplexers are used for different communication applications including satellite communication system and mobile telephony. This approach has two advantages; enabling the use of one antenna by multiple transmitters and hence provide space and reduce the mass on the communications system. However, designing the diplexer circuit is challenging as it needs to have high isolation and low insertion loss to avoid the interference and to achieve the desired function. In addition, wire antennas can be loaded with an LC circuit that can act as a passband or stopband filter at certain frequencies allowing for dual band operation. The dipole and monopole antenna designs of [39] and [42] used the diplexer and LC loading technique which allows each antenna to operate at VHF and UHF bands for CubeSat

communication with ground stations. This is important as it provides more space and less mass on the CubeSat.

D. CIRCULAR POLARIZATION

1) CORNER-TRUNCATED AND SEQUENTIAL-FEEDING

One of the challenges in space communications is polarization mismatch and signal attenuation which can be alleviated by using circular polarized antennas. This is because circular polarization (CP) renders the up/downlink or the intersatellite communication insensitive to antenna misalignment. Especially for the communication between CubeSats and ground stations when a signal is transmitted through the atmosphere, the effect of "Faraday rotation" can be eliminated by using CP antennas at the terminals [88]. The concept behind achieving CP is to excite two orthogonal modes with 90° phase difference and equal amplitude around the resonant frequency [89]. One important metric is the Axial Ratio (AR) bandwidth which shows the polarization purity with respect to frequency and must stay below 3dB. The two most popular approaches that have been adopted by the CubeSat antenna designers are the sequential feeding and the corner truncation which are mainly applied to single patch antennas, patch antenna arrays or reflectarray feeds. The use of square patches with truncated corners can introduce control over the dimensions of the patch to generate the two quadrature orthogonal modes required for CP radiation when fed at the appropriate location. On the other hand, CP radiation can also be achieved by sequentially feeding the individual patches, in the case of patch arrays, with 90° phase difference. This requires a sequential-phase feeding network where the phase at port 1 varies by 90^0 in respect to port 2 and so on. Power dividers such as the Wilkinson power divider containing impedance transformers with delay lines is a popular solution, achieving high isolation between output ports and good matching [14]. One of the main considerations when using sequential-phase feeding is the loss associated with the feedlines which can deteriorate the overall efficiency of the antenna [27].

2) POLARIZER

Most of the high-gain CubeSat antennas are accomplished by using reflector antennas with CP horn feeds. To achieve CP, polarizers are used at the feeds with an Orthomode Transducer (OMT). To generate a CP wave using an OMT, a dual-input source is required that may exceed the complexity and volume permitted by the CubeSat standards [48]. For this reason, the polarizer OMT must be custom made to fit in the antenna stowage volume [49] or it can be realized without OMT by integrating the polarizing structure (cavities) in the horn waveguide [48]. Moreover, polarizers with horn antennas are easier to be realized and used at higher frequencies in the mm-wave domain. The design of a CP feed-polarizer system is of great significance for the performance of reflector antennas as it dictates the AR bandwidth and can minimize the edge diffractions by keeping the edge taper around −10 dB.

VIII. QUALITATIVE EVALUATION

While the previous sections looked at the antenna through their types, in this section, we provide a qualitative comparison of different types of proposed antenna designs for use on CubeSats at different operating frequency bands. Table 11 summarizes their features and performance in terms of operating frequency band, size, bandwidth, gain, reflection coefficient and deployability. Antennas are classified based on their operating frequency and we can see that most proposed antennas are planar (e.g., patch and slot) antennas and operate in the 2.4-2.5 GHz S-band. This is because planar antennas (e.g., patch and slot) are cheap, easy to fabricate and do not require deployment. Moreover, the 2.4-2.5 GHz band is the unlicensed Industrial, Scientific and Medical (ISM) band, meaning the end user is not required obtain a government permit to use the antenna.

A. VHF-BAND ANTENNAS

All VHF-band antenna designs listed in Table 11 are deployable, do not have steering capability, provide low gain and narrow bandwidth. The deployment mechanism incurs extra cost and complexity. Also, there is a risk that the antenna might not deploy, which contributes to the likelihood of mission failure. The helical antenna design in [55], achieves the higher gain of 4.7 dBi at 350 MHz and wider bandwidth of 6% as compared to [39], [42]. However, its size is large, i.e., exceeds 200 mm, and is suitable only for 3U CubeSats. In terms of reflection confection (S_{11}), the monopole design of [42] has the smallest reflection confection, i.e., −35 dB at operating frequency of 144 MHz, however, its bandwidth is very narrow, i.e., 4.86%.

B. UHF-BAND ANTENNAS

In Table 11, there are 10 antenna designs that operate in UHF-band that are suitable for CubeSat communication. These antenna types are slot, dipole, monopole, helical, Yagi-Uda and meander-line antennas. Amongst all UHF-band antenna designs listed in Table 11, only the slot antenna design presented in [35] does not require deployment and hence it does not add extra cost and complexity. Compared to the designs of [35], [39], [42], [52], [53], [55], [56], [72], the Yagi-Uda antenna design of [70] has the highest gain, i.e. 11.5 dBi at 435 MHz. Moreover, the monopole antenna design of [42] has the smallest reflection coefficient of −42 dB as compared to other UHF-band designs in [35], [39], [42], [52], [53], [55], [56]. This shows the antenna achieves good impedance matching and hence most of the power is radiated into space. However, its main limitation is the resulting low gain, e.g., 4.3 dBi. The helical antenna design in [52] provides higher gain of 8.44 dBi at 550 MHz and wider bandwidth of 78.7% as compared to the designs of [35], [39], [42], [53], [55], [56].

C. L-BAND ANTENNAS

Table 11 presents only one L-band patch antenna [21] that was proposed for 3U CubeSat communication. The proposed

TABLE 11. Comparison between all types of proposed antennas for CubeSat based on their operating frequency.

Ref	Operating Frequency (GHz)	Size (λ0 × λ0)	Bandwidth |S11| < -10 dB (%)	Gain (dBi)	S11 (dB) at Center Frequency	Antenna type	Deployable	CubeSat Type	Fabricated	Band
[39]	0.146	0.26	13.7	2.06	-18.5	Dipole	Yes	3U	✔	VHF-Band
[42]	0.144	1.42	8.68	2.59	-14.5	Dipole	Yes	1U	✘	
[42]	0.144	0.45	4.86	2.14	-35	Monopole	Yes	1U	✘	
[55]	0.270	0.35×0.35	6.15	3.56	-19	Helical	Yes	3U	✘	
[55]	0.350	0.35×0.35	6	4.7	-19	Helical	Yes	3U	✘	
[35]	0.485/0.500	n/a	n/a	4	-29	Slot	No	1.5U	✘	UHF-Band
[39]	438	0.26	6.85	3.35	-21	Dipole	Yes	3U	✔	
[42]	435	1.42	5	3.91	-15	Dipole	Yes	1U	✘	
[42]	435	0.45	5.98	4.35	-42	Monopole	Yes	1U	✘	
[52]	0.550	0.22×0.22	78.7	8.44	-20	Helical	Yes	3U	✘	
[53]	0.400	1.83x0.47	n/a	13	n/a	Helical	Yes	1.5U	✔	
[55]	0.450	0.35×0.35	4.67	5.41	-19	Helical	Yes	3U	✘	
[56]	0.365	0.1 ×0.12	7.12	8.38	-27	Helical	Yes	6U	✔	
[70]	0.435	n/a	12.18	11.5	-19	Yagi-Uda	Yes	1.5U	✔	
[72]	0.437	2.52×1.24	5	4.1	-22	Meanderline	Yes	n/a	✘	
[21]	1.57	0.80×0.80	9.55	6	-27	Patch	No	3U	✔	L-Band
[14]	2.45	0.78×0.78	44.90	8.22	- 45	Patch	No	3U	✔	S-Band
[15]	2.43	0.23×0.35	1.65	5.3	-14.5	Patch	No	3U	✔	
[16]	2.45	0.19×0.20	2.45	4.8	-19	Patch	No	1U	✔	
[19]	2.45	0.27×0.72	45.75	8.5	-32.5	Patch	No	3U	✘	
[20]	3.6	1.2×1.2	n/a	30.5	n/a	Patch	Yes	6U	✔	
[21]	2.2	0.80×0.80	9.66	5.4	-40	Patch	No		✔	
[22]	2.43	0.81×0.81	2.67	7.2	-16	Patch	No	1U	✔	
[25]	2.45	0.70×0.70	33.01	4	-22	Patch	No	3U	✔	
[26]	2.25	0.75×0.75	11.11	4.87	-18.5	Patch	No	3U	✘	
[36]	2.45	0.73×0.73	30.20	9.71	-21	Slot	No	3U	✔	
[37]	2.45	0.29×0.29	4.45	8.62	-30	Slot	No	2U	✘	
[38]	2.44	0.31×0.31	2.05	5.8	-34	Slot	No	1U	✔	
[40]	2.45	0.66×0.66	4.8	5.03	-27.35	Dipole	No	1U	✘	
[41]	2.45	0.45×0.45	33.46	3.49	-27.5	Dipole	No	1U	✘	
[24]	2.52	0.67×1.51	11.11	5.2	.23.5	Patch	No	3U	✔	
[65]	2.45	0.72×0.72	n/a	25	n/a	Inflatable	Yes	3U	✘	
[28]	2.30	0.46×0.20	28.70	4.39	-40	Patch	Yes	1U	✘	
[71]	2.47	n/a	5.42	6.41	- 26.47	Yagi-Uda	No	3U	✘	
[13]	5.1	1.41×1.17	10.20	5.9	-17	Patch	No	1U	✘	C-Band
[17]	5.8	1.93×1.93	1.2	6.98	-21	Patch	No	1U	✘	
[18]	8	2.13×2.13	2.39	6.45	-19	Patch	No	3U	✔	
[34]	5	1.18×0.39	1.99	4.98	-17	Slot	No	1U	✔	
[54]	8	3.2×0.8	62.5	12	n/a	Helical	Yes	6U	✘	
[11]	8.25	n/a	16.97	13	-40	Patch	No	1U	✘	X-Band
[12]	7.4	n/a	16.21	7.2	-13	Patch	No	1U	✔	
[18]	11.2	2.13×2.13	3.22	5.34	-15.5	Patch	No	3U	✔	
[23]	10	3.33×3.33	40	15	-18	Patch	No	1U	✔	
[46]	8.425	9.34×5.58	n/a	28	n/a	Reflector	Yes	6U	✔	
[47]	8.425	5.58×9.40	n/a	29.2	n/a	Reflectarray	Yes	6U	✔	
[66]	10	2×4	11.11	17.5	-23	Horn	Yes	6U	✘	
[27]	8.2	2.73×2.73	15.85	20.03	-15	Patch	No	1U	✘	
[49]	8.45		n/a	36.8	n/a	Reflector	Yes	12U	✔	
[50]	8.4	42.8×42.8	n/a	39.6	n/a	Reflectarray	Yes	6U	✔	
[57]	12.2	0.73×0.73	15.57	8.5	-22.5	Helical	No	1U	✔	Ku-Band
[45]	34	56.70	n/a	42.8	n/a	Reflector	Yes	6U	✔	K\Ka-Band
[46]	26	29.38×7.15	n/a	33	n/a	Reflectarray	Yes	3U	✔	
[49]	7.1675 8.435 32 34.45		n/a	36.1 dBic 36.8 dBic 48.7 dBic 48.4 dBic	n/a	Reflector	Yes	12U	✔	
[73]	32	5 (radius)	6.35	24.4	-17	Metasurface	No	1U	✔	
[48]	86	28.73×28.73	9.88	34.36	-24	Reflector	No	6U	✔	W-Band
[74]	94	56×56	2.12	31.9	< -15	Metasurafce	No	1U	✔	

TABLE 11. *(Continued.)* Comparison between all types of proposed antennas for CubeSat based on their operating frequency.

[67]	140, 249, 309	n/a	n/a	20	n/a	Horn	No	3U	✗		mm and sub-mm-Band
[68]	165, 176, 180, 183	n/a	n/a	16-18	n/a	Reflector	No	6U	✓		
[69]	883	58.9	n/a	n/a	n/a	Reflector	No	3U	✓		

dual band antenna provides a total gain of 6 dBi, has small reflection coefficient of −27 dB at 1.57 GHz (band 1) with −10 dB bandwidth of 9.55%. We see that the antenna has a large size of 110 mm × 110 mm as it operates at low frequency. Because of it is large size, the proposed antenna is proposed for 3U CubeSats and it is not suitable for 1U CubeSat. The proposed antenna also operates in the S-band, i.e., 2.2 GHz and provides good performance which will be listed and discussed in next section.

D. S-BAND ANTENNAS
There are 18 S-band antenna designs listed in Table 11 proposed for CubeSat communications. Most of the proposed S-band antennas operate in the unlicensed Industrial, Scientific and Medical (ISM) band (e.g., 2.4-2.5 GHz), are patch antennas and do not require deployment mechanism. Moreover, they provide gains ranging from 4 to 30.5 dBi, −10 dB bandwidths ranging from 1.65 to 45.75% and reflection coefficients (S_{11}) from −16 to −45 dB. Compared to all S-band antenna designs presented in Table 11, the deployable patch antenna array design of [20] provides the highest gain, i.e. 30.5 dBi at 3.6 GHz. However, this antenna design has a large profile and is suitable only for 6U CubeSats as it has a large stowage volume. Amongst all S-band antenna designs listed in Table 11 below, the F-shaped patch antenna design in [19] and the patch antenna array in [14] achieve the widest bandwidths of 45.75% and 44.9%, respectively. The patch antenna array design in [14], also reported the smallest reflection coefficient of −45 dB at 2.45 GHz as compared to all S-band antenna designs in [15], [16], [19]–[22], [24]–[26], [36]–[38], [40]. In terms of antenna size, the meshed patch antenna design of [16], has the smallest size of 24.1 mm × 24.8 mm. Its main limitation, however, is its low gain of 4.8 dBi at 2.45GHz and narrow bandwidth of 2.45%.

E. C-BAND ANTENNAS
For C-band antennas proposed for CubeSat communications, there are only 5 antenna designs [13], [17], [18], [34], [54] listed in Table 11. These C-band antennas provide total gains ranging from 4.98 to 12 dBi, operating frequency range from 5 to 8 GHz, −10 dB bandwidths ranging from 1.2 to 62.5% and reflection coefficients (S_{11}) from −17 to −21 dB. Moreover, all these C-band antennas do not require deployment except the helical antenna design of [54]. Compared to C-band antenna designs in [13], [17], [18], [34], the one

reported in [54] has higher gain, i.e 12 dBi at 6 GHz and a much wider bandwidth, i.e., 62.5%. Compared to the designs of [13], [17], [18], [54], the slot antenna array design in [34], has the smallest size of 70.5 mm × 23.5 mm.

F. X-BAND ANTENNAS
As set out in Table 11, the proposed X-band antenna designs provide gains ranging from 5.3 to 39.6 dBi, operating at a frequency range from 7.4 to 11.2 GHz, −10 dB wide bandwidths ranging from 360.64 to 4000 MHz and reflection coefficients (S_{11}) ranging from −13 to −40 dB. Amongst all X-band antennas designs listed in Table 11, only the designs in [46], [47], [49], [50], [66] are deployable. More specifically, the mesh reflector [49] and reflectarray [50] antennas provide the highest gains of 36.8 and 39.6 dBi at 8.4 GHz respectively. However, they have large sizes and hence they are proposed for 6U and 12U CubeSats. Compared to X-band antenna designs proposed for CubeSat in [11], [12], [18], [46], [47], [66], the antenna design of [23], has much wider bandwidth, i.e. 40%. In terms of reflection coefficient, the patch antenna array design presented in [11], provides the smallest reflection coefficient of −40 dB at 8.25 GHz as compared to all X-band antenna designs listed in Table 11.

G. KU-BAND ANTENNAS
The printed Monofilar square spiral antenna in [57], is the only Ku-band antenna design for CubeSat listed in Table 11. It provides a gain of 8.5 dBi at an operating frequency of 12.2 GHz, wide −10 dBi bandwidth, i.e., 15.57% and small reflection coefficient of −22.5 dB. It also has a small size of 18 mm × 18 mm, hence, it is suitable for use on standard 1U CubeSats.

H. K/Ka-BAND ANTENNAS
In [45], [46], [49] and [73], the authors propose high gain K/Ka-band reflector, reflectarray and metasurface antenna designs respectively. These antenna designs are proposed for different CubeSat sizes ranging from 1U to 12U. Moreover, amongst all K/Ka-band antennas listed in Table 11, only the designs of [45], [46], [49] are deployable. The antenna design of [49] provides the highest gain of 48.7 dBic at operating frequency of 32 GHz. To date, the designs in [45], [46] and [73] are the only K/Ka-band designs that are proposed for CubeSat deep space missions.
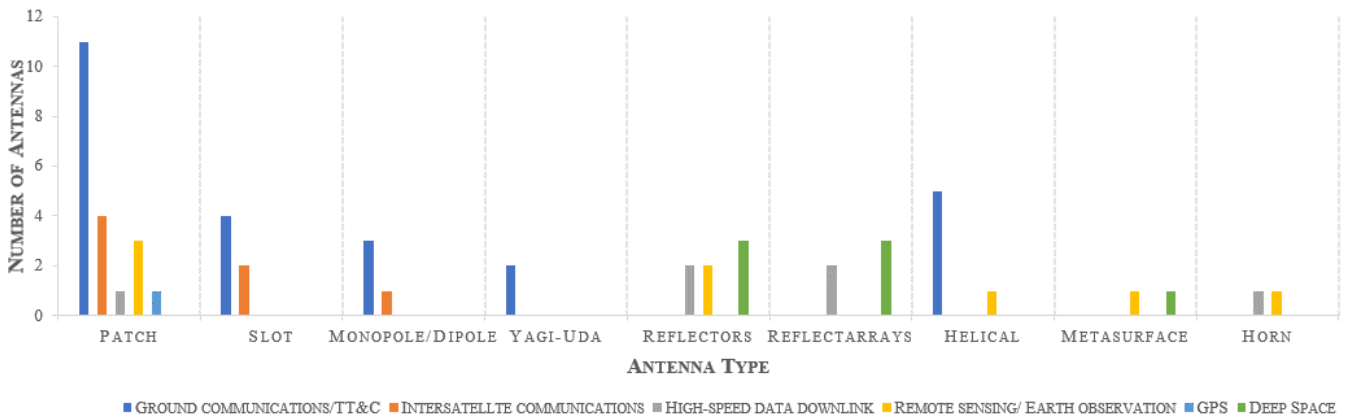
FIGURE 61. Suitability of each antenna type according to the intended CubeSat application.

I. W-BAND ANTENNAS

As set out in Table 11, there are two W-band proposed antennas for CubeSat, which include the feed horn reflector antenna design [48] and the holographic metasurface antenna design [74]. Both designs are not deployable and provide superior gains higher than 30 dBi. The design of [48] is proposed for 6U CubeSat and used reflector antenna while the design of [74] is proposed for 1U CubeSat and used metasurface antenna. Compared to [74], the design of [48], has higher gain and smaller reflection coefficient.

J. mm AND sub-mm-BAND ANTENNAS

Some antenna designs proposed for CubeSat remote sensing applications operate in the millimeter and submillimeter wave bands. Table 11 presents two mm-band horn antennas [67], [68] and one submm-band reflector antenna [69]. The proposed antennas are part of CubeSat radiometer and polarimeter systems that are suitable for 3U and 6U. These antennas have different operating frequencies ranging from 140 to 886GHz and provide gains ranging from 16 to 20 dBi.

IX. DISCUSSION
A. CRITICAL ANALYSIS

From the existing literature the following antenna types are considered as suitable candidates for CubeSat missions, namely planar, slot, monopole/dipole, reflectors, reflectarrays, horns, Yagi-Udas, metasurface and helical antennas. Those antenna types have been used and proposed for a variety of applications by the CubeSat community such as, ground communication or TT&C, intersatellite communications, high-speed data downlinks, remote sensing, GPS and deep space missions. The suitability and frequency of usage of each antenna type according to the intended application is given in Fig. 61. It is obvious that low or medium gain patch, slot, helical, monopole and dipole antennas are the most popular solutions when it comes to ground and intersatellite communications. On the other hand, to establish high-speed data downlinks, high gain antennas are preferred

such as reflectors and reflectarrays. Moreover, only one patch antenna was found that was proposed for GPS application on CubeSat. Besides, CubeSats have been considered for remote sensing applications where horns, reflectors and metasurface antennas operating at mm and sub-mm-wave bands are the most suitable candidates. The most prevailing antenna types for deep space missions are the inflatable or mesh reflectors, the reflectarrays and the all-metal metasurface antennas.

The current CubeSat antenna design's challenges were found to be high gain, wideband, multi band, low profile, and CP. Several techniques were identified that can address those challenges which can be applied either on a single or multiple antenna categories as outlined on Table 10. The most popular technique that can be used to increase the gain is the cavity technique and the use of inflatable, foldable or flexible structures. The cavity approach is more suitable for slot and helical antennas, while the inflatable, foldable or flexible structures can be applied to patch helical, reflectors and reflectarrays. To improve the bandwidth of CubeSat antennas, the most attractive technique was found to be the aperture coupled feeding and the stacked patches while in the case of reflectarrays the subwavelength periodicity can increase the gain bandwidth. Another challenge of high importance is the reduction of the size and mass of the antenna. In this case, the concept of patch, slot and Yagi-Uda antennas integrated with solar panels was the most prominent approach. This approach has an additional benefit of sharing the CubeSat real estate among the antenna and the solar cell subsystems. In addition, achieving CP on CubeSat antennas is a stringent requirement to ensure reliable communication links. Therefore, the most widely used approach by CubeSat designers is the corner truncated patches which can also be applied to reflectarray feeds and the sequential feeding which can be used in conjunction with microstrip antenna arrays.

A qualitative evaluation was performed where factors such as gain, bandwidth, and reflection coefficient at each operating frequency were compared. In addition, the effect of the antenna size and the deployment mechanism was taken

into consideration during the qualitative comparison. It was discovered that planar antennas operating at S- or C-band are the most popular antenna candidates for CubeSat communication. The main advantages are their low profile, low cost, and their beam steering capabilities in the case of patch antenna arrays. Furthermore, most of the planar antennas would not require a deployment mechanism which greatly simplifies the antenna integration with the CubeSat. On the other hand, the most promising antenna type for deep space missions would be Ka-band and X-band reflector, reflectarray and metasurface antennas due to their superior gain performance. UHF and VHF bands are mainly implemented using either helical or monopole/dipole antennas which present a large size and require a deployment mechanism.

B. FUTURE TRENDS

The future of CubeSat antenna designs will be mainly driven by emerging CubeSat applications. These applications include both communications e.g., 5G hybrid satellite-terrestrial (5G S-T) architectures, Internet of Space Things (IoST), Low Earth Orbit Internet of Things (LEO IoT), and scientific such as remote sensing and interplanetary exploration [9], [10], [90]. Therefore, those applications would require CubeSats that can form and maintain cooperative LEO mega constellations and can realize deep space missions.

To achieve the aforementioned requirements while keeping a small form factor and low mass, antennas need to operate in the mm-wave and sub-mm-wave frequency ranges. This would unlock and expand the current CubeSat capabilities by introducing multibeam and beam steering functionalities as indicated by the recent holographic flat-panel metasurface antenna that operates at W-band [74]. In addition, metasurface based antennas at those frequencies can be implemented in silicone-based substrates by using SIW technology and the concept of pillbox beamformer. This

means that they can be integrated with other active electronic components such as amplifiers or mixers. Furthermore, all metal metasurface antennas represent another major candidate for future CubeSat missions especially in deep space [73]. The absence of the dielectric material makes the antenna immune to dielectric losses, hence it can survive the harsh deep space environment. Moreover, by introducing the concept of modulated surface reactance both the aperture field and the polarization of the antenna can be controlled. The last antenna candidate that we believe will play a major role in future CubeSat applications are reconfigurable reflectarrays. To date, reflectarrays have been used on CubeSats by NASA to obtain high gain pencil beams [46], [47], [50]. In addition, reflectarrays can also be used to provide polarization diversity and frequency reuse which is a feature that can greatly increase the current throughput of CubeSats [91]. The next step would be to attempt electronically reconfigurable reflectarray architectures by using PIN diodes, varactor diodes, liquid crystals (LCs) or graphene that can achieve electronic beam scanning [92]. This would allow CubeSats to

establish high gain reconfigurable intersatellite and ground links that are vital for LEO mega constellations. The main drawback of reconfigurable reflectarrays is their limited gain bandwidth which can be lower than 4%. Hence, an interesting combination that can be explored in future CubeSat implementations is the concept of tightly coupled reflectarray antennas [93]. Finally, the antenna will be a critical design aspect of future CubeSat missions. The design and integration of antennas must be considered through the mission design cycle which involve modelling and optimization of antennas along with the satellite structure. Likewise, the fabrication of antennas is also a significant factor where 3D printing technologies can be utilized to lower the cost and accelerate the prototyping process.

Finally, it has been noticed that some antennas for CubeSat were designed to operate at different operating frequency bands without considering the radio regulations provided by International Telecommunication Union (ITU) and Federal Communication Commission (FCC) which control the radio spectrum and frequency bands allocations [94]. Therefore, any antenna designs for space applications should consider the ITU and FCC regulations for frequency and radiation patterns to avoid interference.

X. CONCLUSION

In this paper, we have presented a comprehensive survey of different proposed antenna designs for CubeSats. Firstly, the antennas were categorized according to their type. Their individual performance was analyzed in terms of gain, bandwidth, reflection coefficient, size, and the requirement of a deployment mechanism. The applications of each presented antenna design were listed and discussed. Moreover, the proposed approaches to address the current CubeSat antenna design's challenges such as high gain, wideband, multi band, low profile and CP are analyzed. The reviewed antennas were then classified and evaluated based on their operating frequencies. To conclude, the choice of the antenna type would be dictated by many factors such as the operating frequency, the gain and bandwidth requirements of the mission and the available area on the CubeSat for antenna installation.

REFERENCES

[1] R. Sandau, "Status and trends of small satellite missions for earth observation," *Acta Astronautica*, vol. 66, nos. 1–2, pp. 1–12, Jan. 2010.

[2] C.-C. Liu, "Processing of FORMOSAT-2 daily revisit imagery for site surveillance," *IEEE Trans. Geosci. Remote Sens.*, vol. 44, no. 11, pp. 3206–3214, Nov. 2006.

[3] P. Li, J. Liang, and X. Chen, "Study of printed elliptical/circular slot antennas for ultrawideband applications," *IEEE Trans. Antennas Propag.*, vol. 54, no. 6, pp. 1670–1675, Jun. 2006.

[4] F. E. Tubbal, R. Raad, and K.-W. Chin, "A survey and study of planar antennas for pico-satellites," *IEEE Access*, vol. 3, pp. 2590–2612, 2015.

[5] K. Nakaya, K. Konoue, H. Sawada, K. Ui, H. Okada, N. Miyashita, M. Iai, and S. Matunaga, "Tokyo tech Cubesat: CUTE-I-design & development of flight model and future plan," in *Proc. 21st Int. Commun. Satell. Syst. Conf. Exhib.*, Apr. 2003, p. 2388.

[6] F. E. M. Tubbal, R. Raad, K.-W. Chin, and B. Butters, "S-band planar antennas for a CubeSat," *Int. J. Electr. Eng. Informat.*, vol. 7, no. 4, pp. 559–568, Dec. 2015.

[7] Y. Rahmat-Samii, V. Manohar, and J. M. Kovitz, "For satellites, think small, dream big: A review of recent antenna developments for CubeSats," *IEEE Antennas Propag. Mag.*, vol. 59, no. 2, pp. 22–30, Apr. 2017.

[8] A. H. Lokman, P. J. Soh, S. N. Azemi, H. Lago, S. K. Podilchak, S. Chalermwisutkul, M. F. Jamlos, A. A. Al-Hadi, P. Akkaraekthalin, and S. Gao, "A review of antennas for picosatellite applications," *Int. J. Antennas Propag.*, vol. 2017, pp. 1–17, Apr. 2017.

[9] S. Gao, Y. Rahmat-Samii, R. E. Hodges, and X.-X. Yang, "Advanced antennas for small satellites," *Proc. IEEE*, vol. 106, no. 3, pp. 391–403, Mar. 2018.

[10] N. Chahat, E. Decrossas, D. Gonzalez-Ovejero, O. Yurduseven, M. J. Radway, R. E. Hodges, P. Estabrook, J. D. Baker, D. J. Bell, T. A. Cwik, and G. Chattopadhyay, "Advanced CubeSat antennas for deep space and earth science missions: A review," *IEEE Antennas Propag. Mag.*, vol. 61, no. 5, pp. 37–46, Oct. 2019.

[11] R. Lehmensiek, "Design of a wideband circularly polarized 2 × 2 array with shorted annular patches at X-band on a CubeSat," in *Proc. Int. Symp. Antennas Propag. (ISAP)*, Oct. 2017, pp. 1–2.

[12] J. M. L. Coll, "X-band antenna for CubeSat satellite," B.S. thesis, Lab. Electromagn. Antennas, Universitat Politècnica de Catalunya, Barcelona, Spain, 2017.

[13] M. A. Maged, F. Elhefnawi, H. M. Akah, and H. M. El-Hennawy, "C-band transparent antenna design for intersatellites communication," *Int. J. Sci. Eng. Res.*, vol. 9, no. 3, pp. 248–252, Mar. 2018.

[14] A. Nascetti, E. Pittella, P. Teofilatto, and S. Pisa, "High-gain S-band patch antenna system for earth-observation CubeSat satellites," *IEEE Antennas Wireless Propag. Lett.*, vol. 14, pp. 434–437, Nov. 2015.

[15] N. Neveu, M. Garcia, J. Casana, R. Dettloff, D. R. Jackson, and J. Chen, "Transparent microstrip antennas for CubeSat applications," in *Proc. IEEE Int. Conf. Wireless Space Extreme Environ.*, Nov. 2013, pp. 1–4.

[16] S. K. Podilchak, D. Comite, B. K. Montgomery, Y. Li, V. G.-G. Buendía, and Y. M. M. Antar, "Solar-panel integrated circularly polarized meshed patch for cubesats and other small satellites," *IEEE Access*, vol. 7, pp. 96560–96566, 2019.

[17] R. M. Rodríguez-Osorio and E. F. Ramírez, "A hands-on education project: Antenna design for inter-CubeSat communications [education column]," *IEEE Antennas Propag. Mag.*, vol. 54, no. 5, pp. 211–224, Oct. 2012.

[18] F. Franzén, H. Hultin, and J. Olsson, "A transparent dual-band Cubesat antenna based on stacked patches," B.S. Thesis, School Electr. Eng., KTH Roy. Inst. Technol., Stockholm, Sweden, 2017.

[19] S. Abulgasem, F. Tubbal, R. Raad, P. I. Theoharis, S. Liu, and M. U. A. Khan, "A wideband metal-only patch antenna for CubeSat," *Electronics*, vol. 10, no. 1, pp. 1–13, Dec. 2020.

[20] P. A. Warren, J. W. Steinbeck, R. J. Minelli, and C. Mueller, "Large, deployable S-band antenna for a 6U CubeSat," in *Proc. AIAA Annu. Small Satell.*, Aug. 2015, pp. 1–7.

[21] Y. Yao, S. Liao, J. Wang, K. Xue, E. A. Balfour, and Y. Luo, "A new patch antenna designed for CubeSat: Dual feed, LS dual-band stacked, and circularly polarized," *IEEE Antennas Propag. Mag.*, vol. 58, no. 3, pp. 16–21, Jun. 2016.

[22] T. Yasin and R. Baktur, "Bandwidth enhancement of meshed patch antennas through proximity coupling," *IEEE Antennas Wireless Propag. Lett.*, vol. 16, pp. 2501–2504, Jul. 2017.

[23] S. Zarbakhsh, M. Akbari, M. Farahani, A. Ghayekhloo, T. A. Denidni, and A.-R. Sebak, "Optically transparent subarray antenna based on solar panel for CubeSat application," *IEEE Trans. Antennas Propag.*, vol. 68, no. 1, pp. 319–328, Jan. 2020.

[24] H. Lobato-Morales, S. Villarreal-Reyes, E. Guerrero-Arbona, E. Martinez-Aragon, R. A. Chávez-Pérez, J. L. Medina-Monroy, and C. A. Figueroa-Torres, "A 2.45-GHz circular polarization closed-loop travelling-wave antenna for cubesats," in *Proc. Int. Conf. Electron., Commun. Comput.*, Feb. 2019, pp. 154–157.

[25] M. J. Veljovic and A. K. Skrivervik, "Aperture-coupled low-profile wideband patch antennas for CubeSat," *IEEE Trans. Antennas Propag.*, vol. 67, no. 5, pp. 3439–3444, May 2019.

[26] A. Ygnacio-Espinoza, D. Penaloza-Aponte, J. Alvarez-Montoya, A. Mesco-Quispe, and M. Clemente-Arenas, "Quasi-transparent meshed and circularly polarized patch antenna with metamaterials integrated to a solar cell for S-band CubeSat applications," in *Proc. Int. Conf. Electromagn. Adv. Appl. (ICEAA)*, Sep. 2018, pp. 605–608.

[27] S. X. Ta, V. D. Le, K. K. Nguyen, and C. Dao-Ngoc, "Planar circularly polarized X-band array antenna with low sidelobe and high aperture efficiency for small satellites," *Int. J. RF Microw. Comput.-Aided Eng.*, vol. 29, no. 11, pp. 1–9, Nov. 2019.

[28] O. F. G. Palacios, R. E. D. Vargas, J. A. H. Perez, and S. B. C. Erazo, "S-band koch snowflake fractal antenna for cubesats," in *Proc. IEEE ANDESCON*, Oct. 2016, pp. 1–4.

[29] T. Shahvirdi and R. Baktur, "Analysis of the effect of solar cells on the antenna integrated on top of their cover glass," in *Proc. IEEE Int. Symp. Antennas Propag. USNC/URSI Nat. Radio Sci. Meeting*, Jul. 2015, pp. 2429–2430.

[30] L. K. Fong and R. Chair, "On the use of shorting pins in the design of microstrip patch antennas," *HKIE Trans.*, vol. 11, no. 4, pp. 31–38, Jan. 2004.

[31] S. Zarbakhsh, M. Akbari, F. Samadi, and A.-R. Sebak, "Broadband and high-gain circularly-polarized antenna with low RCS," *IEEE Trans. Antennas Propag.*, vol. 67, no. 1, pp. 16–23, Jan. 2019.

[32] M. Akbari, M. Farahani, A.-R. Sebak, and T. A. Denidni, "Ka-band linear to circular polarization converter based on multilayer slab with broadband performance," *IEEE Access*, vol. 5, pp. 17927–17937, 2017.

[33] F. E. Tubbal, R. Raad, K.-W. Chin, and B. Butters, "S-band shorted patch antenna for inter pico satellite communications," in *Proc. 8th Int. Conf. Telecommun. Syst. Services Appl. (TSSA)*, Oct. 2014, pp. 1–4.

[34] M. A. Maged, F. El-Hefnawi, H. M. Akah, A. El-Akhdar, and H. M. S. El-Hennawy, "Design and realization of circular polarized SIW slot array antenna for cubesat intersatellite links," *Prog. Electromagn. Res. Lett.*, vol. 77, pp. 81–88, Jul. 2018.

[35] S. Tariq and R. Baktur, "Circularly polarized UHF up- and downlink antennas integrated with CubeSat solar panels," in *Proc. IEEE Int. Symp. Antennas Propag. USNC/URSI Nat. Radio Sci. Meeting*, Jul. 2015, pp. 1424–1425.

[36] F. Tubbal, R. Raad, K.-W. Chin, L. Matekovits, B. Butters, and G. Dassano, "A high gain S-band slot antenna with MSS for CubeSat," *Ann. Telecommun.*, vol. 74, nos. 3–4, pp. 223–237, Apr. 2019.

[37] F. E. Tubbal, R. Raad, and K.-W. Chin, "A low profile high gain CPW-fed slot antenna with a cavity backed reflector for CubeSats," in *Proc. 11th Int. Conf. Signal Process. Commun. Syst. (ICSPCS)*, Dec. 2017, pp. 1–4.

[38] A. J. M. Volkan and O. T. Letters, "Electrically small printed antenna for applications on cubesat and nano-satellite platforms," *Microw. Opt. Technol. Lett.*, vol. 57, no. 4, pp. 891–896, Apr. 2015.

[39] T. F. C. Leao, V. Mooney-Chopin, C. W. Trueman, and S. Gleason, "Design and implementation of a diplexer and a dual-band VHF/UHF antenna for nanosatellites," *IEEE Antennas Wireless Propag. Lett.*, vol. 12, pp. 1098–1101, Sep. 2013.

[40] S. Liu, R. Raad, K.-W. Chin, and F. E. M. Tubbal, "Dipole antenna array cluster for CubeSats," in *Proc. 10th Int. Conf. Signal Process. Commun. Syst. (ICSPCS)*, Dec. 2016, pp. 1–4.

[41] A. H. Lokman, P. J. Soh, S. N. Azemi, M. F. Jamlos, A. A. Al-Hadi, S. Chalermwisutkul, and P. Akkaraekthalin, "Compact circularly polarized S-band antenna for pico-satellites," in *Proc. Int. Symp. Antennas Propag. (ISAP)*, Oct. 2017, pp. 1–2.

[42] K. Schraml, A. Narbudowicz, S. Chalermwisutkul, D. Heberling, and M. J. Ammann, "Easy-to-deploy LC-loaded dipole and monopole antennas for cubesat," in *Proc. 11th Eur. Conf. Antennas Propag. (EUCAP)*, Mar. 2017, pp. 2303–2306.

[43] W. Traussnig, "Design of a communication and navigation subsystem for a CubeSat mission," M.S. thesis, KFU Graz, Graz, Austria, 2007. Accessed: Apr. 20, 2020. [Online]. Available: https://physik.unigraz.at/spacesciences/archive/files/ULG_II_Master_Thesis_Traussnig.pdf

[44] S. Rao, L. Shafai, and S. K. Sharma, *Handbook of Reflector Antennas and Feed Systems Volume III: Applications of Reflectors*. Boston, MA, USA: Artech House, 2013.

[45] N. Chahat, R. E. Hodges, J. Sauder, M. Thomson, E. Peral, and Y. Rahmat-Samii, "CubeSat deployable Ka-band mesh reflector antenna development for earth science missions," *IEEE Trans. Antennas Propag.*, vol. 64, no. 6, pp. 2083–2093, Jun. 2016.

[46] R. E. Hodges, D. J. Hoppe, M. J. Radway, and N. E. Chahat, "Novel deployable reflectarray antennas for CubeSat communications," in *IEEE MTT-S Int. Microw. Symp. Dig.*, May 2015, pp. 1–4.

[47] R. E. Hodges, N. Chahat, D. J. Hoppe, and J. D. Vacchione, "A deployable high-gain antenna bound for Mars: Developing a new folded-panel reflectarray for the first CubeSat mission to Mars," *IEEE Antennas Propag. Mag.*, vol. 59, no. 2, pp. 39–49, Apr. 2017.

[48] G. Mishra, S. K. Sharma, and J.-C. S. Chieh, "A circular polarized feed horn with inbuilt polarizer for offset reflector antenna for *W*-band CubeSat applications," *IEEE Trans. Antennas Propag.*, vol. 67, no. 3, pp. 1904–1909, Dec. 2018.

[49] N. Chahat, J. Sauder, M. Mitchell, N. Beidleman, and G. Freebury, "One-meter deployable mesh reflector for deep-space network telecommunication at *X*-band and *Ka*-band," *IEEE Trans. Antennas Propag.*, vol. 68, no. 2, pp. 727–735, Feb. 2020.

[50] M. Arya, J. F. Sauder, R. Hodges, and S. Pellegrino, "Large-area deployable reflectarray antenna for CubeSats," in *Proc. AIAA Scitech Forum Expo. (SciTech)*, Jan. 2019, p. 2257.

[51] J. D. Kraus, "The helical antenna," *Proc. IRE*, vol. 37, no. 3, pp. 263–272, Mar. 1949.

[52] J. Costantine, Y. Tawk, S. Moth, C. G. Christodoulou, and S. E. Barbin, "A modified helical shaped deployable antenna for cubesats," in *Proc. IEEE-APS Topical Conf. Antennas Propag. Wireless Commun. (APWC)*, Sep. 2012, pp. 1114–1116.

[53] D. Ochoa, K. Hummer, and M. Ciffone, "Deployable helical antenna for nano-satellites," in *Proc. 28th Annu. AIAA/USU Conf. Small Satell.*, 2014, pp. 1–7.

[54] J.-K. Che, C.-C. Chen, and J. T. Johnson, "A 6–40 GHz CubeSAT antenna system," in *Proc. 11th Eur. Conf. Antennas Propag.*, Mar. 2017, pp. 1883–1887.

[55] J. Costantine, D. Tran, M. Shiva, Y. Tawk, C. G. Christodoulou, and S. E. Barbin, "A deployable quadrifilar helix antenna for CubeSat," in *Proc. IEEE Int. Symp. Antennas Propag.*, Jul. 2012, pp. 1–2.

[56] J. Costantine, Y. Tawk, I. Maqueda, M. Sakovsky, G. Olson, S. Pellegrino, and C. G. Christodoulou, "UHF deployable helical antennas for Cube-Sats," *IEEE Trans. Antennas Propag.*, vol. 64, no. 9, pp. 3752–3759, Sep. 2016.

[57] Q. Luo, S. Gao, M. Sobhy, J. Li, G. Wei, and J. Xu, "A broadband printed monofilar square spiral antenna: A circularly polarized low-profile antenna," *IEEE Antennas Propag. Mag.*, vol. 59, no. 2, pp. 79–87, Apr. 2017.

[58] J. D. Lohn, W. F. Kraus, and D. S. Linden, "Evolutionary optimization of a quadrifilar helical antenna," in *Proc. IEEE Antennas Propag. Soc. Int. Symp.*, vol. 3, Jun. 2002, pp. 814–817.

[59] K. Mandal and P. P. Sarkar, "High gain wide-band U-shaped patch antennas with modified ground planes," *IEEE Trans. Antennas Propag.*, vol. 61, no. 4, pp. 2279–2282, Apr. 2013.

[60] W. L. Stutzman and G. A. Thiele, *Antenna Theory and Design*. Hoboken, NJ, USA: Wiley, 2012.

[61] S. G. Ow and P. J. Connolly, "Quadrifilar helix antenna," U.S. Patent 5 349 365, Sep. 20, 1994.

[62] B. Slade, "The basics of quadrifilar helix antennas," Orban Microw., Orlando, FL, USA, Tech. Rep., Mar. 2015, pp. 6–16.

[63] J. M. Tranquilla and S. R. Best, "A study of the quadrifilar helix antenna for global positioning system (GPS) applications," *IEEE Trans. Antennas Propag.*, vol. 38, no. 10, pp. 1545–1550, Oct. 1990.

[64] Y.-S. Wang and S.-J. Chung, "A miniature quadrifilar helix antenna for global positioning satellite reception," *IEEE Trans. Antennas Propag.*, vol. 57, no. 12, pp. 3746–3751, Dec. 2009.

[65] A. Babuscia, B. Corbin, M. Knapp, R. Jensen-Clem, M. Van de Loo, and S. Seager, "Inflatable antenna for cubesats: Motivation for development and antenna design," *Acta Astronautica*, vol. 91, pp. 322–332, Oct. 2013.

[66] A. Gupta, J. Costantine, Y. Tawk, C. G. Christodoulou, S. Pellegrino, and M. Sakovsky, "A deployable vivaldi-fed conical horn antenna for CubeSats," in *Proc. United States Nat. Committee URSI Nat. Radio Sci. Meeting (USNC-URSI NRSM)*, Jan. 2016, pp. 1–2.

[67] B. R. Johnson, C. J. Vourch, T. D. Drysdale, A. Kalman, S. Fujikawa, B. Keating, and J. Kaufman, "A CubeSat for calibrating ground-based and sub-orbital millimeter-wave polarimeters (CalSat)," *J. Astronomical Instrum.*, vol. 4, nos. 3–4, Dec. 2015, Art. no. 1550007.

[68] S. C. Reising, T. C. Gaier, C. D. Kummerow, V. Chandrasekar, S. T. Brown, S. Padmanabhan, B. H. Lim, S. C. van den Heever, T. S. L'Ecuyer, C. S. Ruf, Z. S. Haddad, Z. J. Luo, S. J. Munchak, G. Berg, T. C. Koch, and S. A. Boukabara, "Overview of temporal experiment for storms and tropical systems (TEMPEST) CubeSat constellation mission," in *IEEE MTT-S Int. Microw. Symp. Dig.*, Phoenix, AZ, USA, May 2015, pp. 1–4.

[69] J. Esper, D. Wu, B. Abresch, B. Flaherty, C. Purdy, J. Hudeck, J. Rodriguez, and T. Daisey, "NASA IceCube: CubeSat demonstration of a commercial 883-GHz cloud radiometer," in *Proc. 32nd Annu. AIAA/USU Conf. Small Satell.*, Salt Lake City, UT, USA, Aug. 2018, pp. 1–15.

[70] W. Alomar, J. Degnan, S. Mancewicz, M. Sidley, J. Cutler, and B. Gilchrist, "An extendable solar array integrated Yagi-Uda UHF antenna for Cube-Sat platforms," in *Proc. IEEE Int. Symp. Antennas Propag. (APSURSI)*, Jul. 2011, pp. 3022–3024.

[71] S. Liu, R. Raad, and F. E. M. Tubbal, "Printed Yagi-Uda antenna array on CubeSat," in *Proc. 11th Int. Conf. Signal Process. Commun. Syst. (ICSPCS)*, Dec. 2017, pp. 1–5.

[72] A. H. Lokman, P. J. Soh, S. N. Azemi, H. Lago, M. A. I. Yatim, M. E. A. Aziz, and A. A. Al-Hadi, "A flexible deployable CubeSat antenna," in *Proc. IEEE Asia–Pacific Conf. Appl. Electromagn. (APACE)*, Dec. 2016, pp. 1–17.

[73] D. Gonzalez-Ovejero, N. Chahat, R. Sauleau, G. Chattopadhyay, S. Maci, and M. Ettorre, "Additive manufactured metal-only modulated meta-surface antennas," *IEEE Trans. Antennas Propag.*, vol. 66, no. 11, pp. 6106–6114, Nov. 2018.

[74] O. Yurduseven, C. Lee, D. Gonzalez-Ovejero, M. Ettorre, R. Sauleau, G. Chattopadhyay, V. Fusco, and N. Chahat, "Multi-beam Si/GaAs holographic metasurface antenna at W-band," *IEEE Trans. Antennas Propag.*, early access, Oct. 20, 2020, doi: 10.1109/TAP.2020.3030898.

[75] B. G. Evans, *Satellite Communication Systems*, 3th ed. London, U.K.: IET, 1999.

[76] D. M. Pozar and S. M. Duffy, "A dual-band circularly polarized aperture-coupled stacked microstrip antenna for global positioning satellite," *IEEE Trans. Antennas Propag.*, vol. 45, no. 11, pp. 1618–1625, Nov. 1997.

[77] F. Xu and K. Wu, "Guided-wave and leakage characteristics of substrate integrated waveguide," *IEEE Trans. Microw. Theory Techn.*, vol. 53, no. 1, pp. 66–73, Jan. 2005.

[78] G. Q. Luo, W. Hong, Q. H. Lai, K. Wu, and L. L. Sun, "Design and experimental verification of compact frequency-selective surface with quasi-elliptic bandpass response," *IEEE Trans. Microw. Theory Techn.*, vol. 55, no. 12, pp. 2481–2487, Dec. 2007.

[79] D. M. Pozar, "Microstrip antenna aperture-coupled to a microstripline," *Electron. Lett.*, vol. 21, no. 1, pp. 49–50, Jan. 1985.

[80] C. Kilgus, "Multielement, fractional turn helices," *IEEE Trans. Antennas Propag.*, vol. AP-16, no. 4, pp. 499–500, Jul. 1968.

[81] C. Kilgus, "Resonant quadrafilar helix," *IEEE Trans. Antennas Propag.*, vol. AP-17, no. 3, pp. 349–351, May 1969.

[82] C. Kilgus, "Shaped-conical radiation pattern performance of the backfire quadrifilar helix," *IEEE Trans. Antennas Propag.*, vol. AP-23, no. 3, pp. 392–397, May 1975.

[83] D. M. Pozar, "Wideband reflectarrays using artificial impedance surfaces," *Electron. Lett.*, vol. 43, no. 3, pp. 148–149, Feb. 2007.

[84] E. Almajali, D. A. McNamara, J. Shaker, and M. R. Chaharmir, "Observations on the performance of reflectarrays with reduced inter-element spacings," in *Proc. IEEE Int. Symp. Antennas Propag. (APSURSI)*, Jul. 2011, pp. 369–372.

[85] T. Yekan and R. Baktur, "Conformal integrated solar panel antennas: Two effective integration methods of antennas with solar cells," *IEEE Antennas Propag. Mag.*, vol. 59, no. 2, pp. 69–78, Apr. 2017.

[86] S.-M. Yang and C.-H. Huang, "An inductor model for analyzing the performance of printed meander line antennas in smart structures," *J. Electromagn. Anal. appl.*, vol. 6, no. 9, p. 244, 2014.

[87] C. Turcu, C. Turcu, and V. Popa, "An RFID and agent technologies based system for the identification and monitoring of patients," in *Proc. 8th Int. Conf. Develop. Appl. Syst.*, May 2006, pp. 234–241.

[88] S. Gao, Q. Luo, and F. Zhu, "Introduction to circularly polarized antennas," in *Circularly Polarized Antennas*. Chechister, U.K.: Wiley, 2014, pp. 1–25.

[89] K.-F. Lee and K.-F. Tong, "Microstrip patch antennas—Basic characteristics and some recent advances," *Proc. IEEE*, vol. 100, no. 7, pp. 2169–2180, Jul. 2012.

[90] N. Saeed, A. Elzanaty, H. Almorad, H. Dahrouj, T. Y. Al-Naffouri, and M.-S. Alouini, "CubeSat communications: Recent advances and future challenges," *IEEE Commun. Surveys Tuts.*, vol. 22, no. 3, pp. 1839–1862, 3rd Quart., 2020.

[91] M. H. Dahri, M. H. Jamaluddin, M. Khalily, M. I. Abbasi, R. Selvaraju, and M. R. Kamarudin, "Polarization diversity and adaptive beamsteering for 5G reflectarrays: A review," *IEEE Access*, vol. 6, pp. 19451–19464, 2018.

[92] P. Nayeri, F. Yang, and A. Z. Elsherbeni, "Beam-scanning reflectarray antennas: A technical overview and state of the art," *IEEE Antennas Propag. Mag.*, vol. 57, no. 4, pp. 32–47, Aug. 2015.

[93] J. Wang, Y. Zhou, S. Gao, and Q. Luo, "An efficiency-improved tightly coupled dipole reflectarray antenna using variant-coupling-capacitance method," *IEEE Access*, vol. 8, pp. 37314–37320, 2020.

[94] S. E. Palo, "High rate communications systems for CubeSats," in *IEEE MTT-S Int. Microw. Symp. Dig.*, May 2015, pp. 1–4.

SUHILA ABULGASEM (Student Member, IEEE) received the B.E. degree from the College of Electronic Technology, Tripoli, Libya, in 2005, and the M.S. degree in information technology from the University of Wollongong, Wollongong, NSW, Australia, in 2013, where she is currently pursuing the Ph.D. degree in telecommunications engineering, under the Australian Government Research Training Program (RTP) scholarship. Her research interests include slot and patch antenna designs for CubeSat applications.
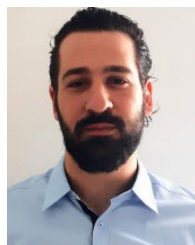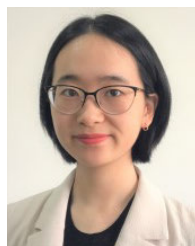
PANAGIOTIS (YANI) IOANNIS THEOHARIS (Student Member, IEEE) was born in Athens, Greece, in 1993. He received the B.Eng. degree (Hons.) in telecommunications engineering from the University of Wollongong, Wollongong, NSW, Australia, in 2018, where he is currently pursuing the Ph.D. degree under the Australian Government Research Training Program (RTP) scholarship. His research interests include antenna design for CubeSat applications, reconfigurable antennas, reflectarray antennas, and wearable antennas.

FAISEL TUBBAL (Senior Member, IEEE) received the B.E. degree from the College of Electronic Technology, Tripoli, Libya, in 2004, and the M.S. degree in telecommunication engineering, the M.S. degree in engineering management, and the Ph.D. degree in telecommunication engineering from the University of Wollongong, Wollongong, NSW, Australia, in 2012, 2013, and 2017, respectively.

He has been working as a Researcher with the Libyan Centre for Remote Sensing and Space Science (LCRSSC), Tripoli. He joined the School of Electrical, Computer and Telecommunication Engineering, University of Wollongong, as an Academic Assistant, in 2012. Since 2017, he has been a casual unit Convenor with the School of Computing, Engineering and Mathematics, Western Sydney University, Australia. He was promoted to the position of Laboratory Manager with the School of Computer, Electrical and Telecommunication Engineering (SECTE), University of Wollongong, in 2019. He is the author of three chapters and more than 40 conference and journal papers. His research interests include antenna designs for CubeSat communications, wearable antennas, reconfigurable antennas, and antenna designs using metamaterials and metasurface antennas. His Ph.D. thesis was entitled S-band Planar Antenna Designs for CubeSat Communications.

Dr. Tubbal is a Fellow of the Wollongong Academy for Tertiary Teaching and Learning Excellence (WATTLE). He was a recipient of the Vice-Chancellor's Awards for Outstanding Contribution to Teaching and Learning (OCTAL).

SINING LU (Student Member, IEEE) received the Bachelor of Engineering degree (Hons.) in telecommunications engineering from the University of Wollongong, Wollongong, NSW, Australia, in 2015, where she is currently pursuing the Doctor of Philosophy degree in telecommunications engineering. Her research interests include design of antennas and antenna arrays for CubeSat and CubeSat swarm applications.

RAAD RAAD (Member, IEEE) received the Bachelor of Engineering degree (Hons.) in electrical engineering from the University of Wollongong, Wollongong, NSW, Australia, in 1997, the master's degree from the Switched Networks Research Centre, University of Wollongong, and the Ph.D. degree in neuro-fuzzy logic admission control in cellular mobile networks, in 2006.

Since 2004, he has been with the School of Electrical, Computer and Telecommunications Engineering, University of Wollongong, where he works as the Deputy Head of the School. His current research interests include wireless communications, CubeSat, the IoT, and antenna design. He received an Australian Postgraduate Award (APA) that was matched by Telstra Research Laboratories (TRL). He received scholarship from the Motorola Australian Research Centre (MARC) in the later part of his degree.

SAEID IRANMANESH received the B.E. and M.S. degrees in computer science from Azad University, Tehran, Iran, and the Ph.D. degree in electrical and telecommunication engineering from the University of Wollongong, Wollongong, NSW, Australia, in 2015. He has been working as a member of the Tele Research Group, School of Electrical, Computer, and Telecommunication Engineering, University of Wollongong. He was appointed as an Assistant Professor with Azad University, for a period of year. He is currently appointed with the Melbourne Institute of Technology, Sydney, NSW. His research interests include wireless networks, intelligent transportation systems, and smart cities. His Ph.D. thesis was entitled as Data Management in Delay Tolerant Networks.

• • •